10-20-2015 12:00 AM

Analysis and Compensation of Power Amplifier Distortions in Wireless Communication Systems

Sharath Manjunath, *The University of Western Ontario*

Supervisor: Dr. Xianbin Wang, *The University of Western Ontario*
Joint Supervisor: Dr. Anestis Dounavis, *The University of Western Ontario*
A thesis submitted in partial fulfillment of the requirements for the Master of Engineering Science degree in Electrical and Computer Engineering

ANALYSIS AND COMPENSATION OF POWER AMPLIFIER DISTORTIONS IN WIRELESS COMMUNICATION SYSTEMS

(Thesis format: Monograph)

by

Sharath Manjunath

Graduate Program in Electrical and Computer Engineering Department

A thesis submitted in partial fulfillment
of the requirements for the degree of
Master of Engineering Science

The School of Graduate and Postdoctoral Studies
The University of Western Ontario
London, Ontario, Canada

Abstract

Wireless communication devices transmit message signals which should possess desirable power levels for quality transmission. Power amplifiers are devices in the wireless transmitters which increase the power of signals to the desired levels, but produce nonlinear distortions due to their saturation property, resulting in degradation of the quality of the transmitted signal. This thesis talks about the analysis and performance of communication systems in presence of power amplifier nonlinear distortions.

First, the thesis studies the effects of power amplifier nonlinear distortions on communication signals and proposes a simplified design for identification and compensation of the distortions at the receiver end of a wireless communication system using a two-step pilot signal approach. Step one involves the estimation of the channel state information of the wireless channel and step two estimates the power amplifier parameters. Then, the estimated power amplifier parameters are used for transmitter identification with the help of a testing procedure proposed in this thesis.

With the evolution of millimeter wave wireless communication systems today, study and analysis of these systems is the need of the hour. Thus, the second part of this thesis is extended to study the performance of millimeter wave wireless communication systems in presence of power amplifier nonlinear distortions and derives an analytical expression for evaluation of the symbol error probability for this system. The proposed analysis evaluates the performance of millimeter wave systems theoretically without the need of complex simulations, and is helpful in studying systems in the absence of actual hardware.

Keywords: Rapp Model, Device Identification, Millimeter waves

Acknowledgments

This thesis would not have been a reality without the support and contributions of a number of people. I would like to sincerely thank all of them. First and foremost, I would like to sincerely thank my supervisors Prof. Xianbin Wang and Prof. Anestis Dounavis for giving me an opportunity to work under them at University of Western Ontario. Their constant supervision and encouragement helped me in reaching greater heights in my career.

I would like to express my sincere gratitude to my colleague Dr. Aydin Behnad, post doctoral fellow at University of Western Ontario for his selfless help and guidance from time to time, in achieving my objectives and working towards the production of this thesis. His patience and time spent in helping me achieving my objectives through timely suggestions is priceless. His motivational words stood by me and boosted my confidence during every step of the technical activities I carried out for the production of this thesis.

My sincere thanks to my research group, colleagues, faculty and staff members, and students of University of Western Ontario who have directly or indirectly helped me in achieving my objectives towards the progression of my thesis.

Last but not the least, I would like to thank my parents Manjunath K N (father), Ushadevi N S (mother) for their love, support and encouragement which enabled me work towards achieving my career objectives. Thanks to my beloved friends of Canada, Vivek, Shankar, Sushek, Sharanjith, Rasika, Karthik, Arthi, Shreyas, Nilesh and others (the list is long), my roommates Shankar, Rohit, Sridhar, Gopi Krishna and my beloved lab-mates Sourajeet (former), Tarek, Mohamed and Sadia for their support and cooperation in London, ON, Canada.

Contents

List of Figures

Acronyms

AM	*Amplitude Modulation*
AM-AM	*Amplitude Modulation-Amplitude Modulation*
AM-PM	*Amplitude Modulation-Phase Modulation*
ASK	*Amplitude Shift Keying*
AWGN	*Additive White Gaussian Noise*
BER	*Bit Error Rate*
DC	*Direct Current*
DVB	*Digital Video Broadcasting*
FFT	*Fast Fourier Transform*
FIR	*Finite Impulse Response*
FM	*Frequency Modulation*
FSK	*Frequency Shift Keying*
GPS	*Global Positioning System*
IBO	*Input Back-Off*
IFFT	*Inverse Fast Fourier Transform*
MIMO	*Multiple Input Multiple Output*
OFDM	*Orthogonal Frequency Division Multiplexing*
PA	*Power Amplifier*
PAPR	*Peak-to-Average Power Ratio*
PSD	*Power Spectral Density*
PSK	*Phase Shift Keying*
QAM	*Quadrature Amplitude Modulation*
RF	*Radio Frequency*
SSPA	*Solid State Power Amplifier*
SEL	*Soft-Envelope Limiter*
SER	*Symbol Error Rate*
TWTA	*Travelling Wave Tube Amplifier*
UHF	*Ultra High Frequency*
3GPP	*Third Generation Partnership Project*

Chapter 1

Introduction

Wireless Communication is becoming an integral part of the modern life. With the first demonstration of transmission of a message signal using 'Hertzian Waves' by Guglielmo Marconi in 1895, technologies in wireless communication has developed many folds to what it is in the present era [1]. Today, wireless communication is applied in many aspects ranging from cellphone, involving communication between two individuals, to mass broadcast of television/radio channels involving a larger group of people. Though initially wireless communication was applied only for military applications, innumerable applications are found today in other fields which include telephony, fax services, AM/FM radios, Digital Video Broadcasting (DVB), Global Positioning Systems (GPS), astronomical experiments etc. Some other specific applications include wireless keyboards and headphones, remote key-less systems to lock vehicles, Wireless Fidelity (Wi-Fi) etc. Presently, research work is done in the application of wireless systems for device to device communication termed 'Smart Devices' which enable the devices to operate interactively.

Wireless communication is preferred over wired communication due to its various advantages like flexibility, mobility, ease of use, easy planning and installation, durability and lower costs. In spite of the advantages, wireless communication systems has its own challenges.

Since, wireless communication has a broadcast nature and uses a frequency spectrum of electromagnetic waves, it has limitations of spectrum availability, limited capacity, service quality uncertainties and compatibility issues [2]. The broadcast nature of wireless communication makes it susceptible to data loss and theft since, these signals are prone to being intercepted by any receiver other than the sole intended one. This opened challenges and scope for developing secured communication mechanisms. Limited spectrum resources led to the concept of frequency re-usability and paved the way for design and development of optimum 'cells' for the purpose without signal interference. Service quality uncertainties are caused because wireless signals are susceptible to distortions due to the transmitter and the wireless channel. These distortions are dependent on the type of signal, its operating frequency, modulation schemes etc. and distortion prevention or compensation mechanisms are adopted in the wireless communication. Compatibility issues arise when two wireless devices operate at different standards, such as different operating frequencies, modulation schemes etc.

Needless to say, wireless communication is still the preferred mode for communication due to its advantages over wired communication. Even though the issues related to wireless communications are currently addressed, they are still not completely resolved and research is being done for improvements. With evolution of wireless technologies from Marconi to 5G, corresponding evolution in compensation mechanisms is also the need of the hour.

1.1 Motivations

In this section, the motivation for the production of this thesis has been presented. The analysis of service quality uncertainties in wireless communications, with a special emphasis on quality deterioration due to power amplifier (PA) nonlinear distortions, is the focus in this

thesis.

Compensation mechanisms have been developed and are put in use for linear distortions due to its simpler implementation in wireless communication but is slightly complex for compensating nonlinear distortions. Nonlinear distortions are mainly caused by the power amplifier component of the transmitter. Due to this, most communication devices adopt methods of preventing the distortion or by using a predistorter at the transmitter [3]. Research work related to nonlinear models and compensation mechanisms is explored in numerous articles, but the complexity of the models is high, leading to intensive signal processing at the transceiver devices which may not be required due to the fairly static nature of the distortions [3]. The complexity is high as the distortions in the received signal is seen as a combined effect of the static nonlinear distortion and the dynamic channel distortions. This motivated to develop a static compensation model with less complexity for the nonlinear distortions in a wireless communication system, separating the dynamic distortions of the channel. The knowledge of this power amplifier nonlinear distortion (which can be defined by a set of parameters) can also be used for identification of the transmitter device as it is specific to the given transmitter.

The challenges further increase when power amplifiers are operated in the millimeter wave range as there are other stray effects on the signal like delay, attenuation, dispersion etc. [4] due to their high frequency operation, and design of compensation models are further cumbersome. Millimeter wave signals, due to their short wavelengths suffer from higher rain attenuation with increase in frequency [5]. The use of power amplifiers for amplification of millimeter wave signals to maintain the desired power levels of the signal, again produce nonlinear distortions. This motivated the need to study the behavior of millimeter wave wireless communication systems in presence of nonlinear distortions, so that the analysis can be used to develop compensation models for the distortions produced. Also, due to limited commercial availability of

hardware for millimeter wave systems, it would be convenient to have mathematical models for performance evaluation of these systems.

With these aspects in mind, research activities were carried out in this direction and the results are given in this thesis.

1.2 Contributions

Various studies on power amplifier nonlinear distortions are studied in literature. With the above mentioned motives, the following are the contributions in this thesis.

- A pilot signal based power amplifier nonlinear distortion compensator for a MIMO-STBC (Multiple Input Multiple Output-Space Time Block Code) system modulated by a QAM (Quadrature Amplitude Modulation) wireless communication systems is designed. In the proposed method, a methodology to identify the source of distortion, its compensation and application in a transmitter device identification process is proposed using a two-step pilot signal approach. Step one involves the estimation of the channel and the step two estimates the transmitter power amplifier parameters which are used to compensate distortions and identify the device. The device identification process involves the comparison of the estimated power amplifier parameters with a validated set of parameters. Results from computer simulation show that the proposed compensation method has a significantly good performance in terms of the bit error rate of the system and successfully identifies the transmitter device. A bit error rate of 1% was achieved for a signal to noise ratio of 25 dB. The proposed method was developed with the intention to reduce the complexity of the distortion compensator by separating out the static nonlinear distortion and the dynamic channel distortion, and identification of the transmitter at

the receiver.

- Considering a millimeter wave Orthogonal Frequency Division Multiplexing (OFDM) wireless communication system, its performance in presence of power amplifier nonlinear distortions is studied in chapter 4. An analytical expression for the symbol error probability has been derived to evaluate the performance of a millimeter wave system in presence of these distortions, which can be used in place of the cumbersome evaluation through complex simulations. The results of the analytical expression is compared to the computer simulated values of a communication system and verified. This analytical expression enables the study of the performance of OFDM systems theoretically and can be used to develop nonlinear compensation models in future work. This is followed by a methodology to obtain the equivalent parameters for the well known Rapp model to study millimeter wave power amplifiers. The motive behind deriving the equivalent parameters is the easier implementation of millimeter wave power amplifiers by fitting it to the currently available models in simulation softwares. Most simulators (like SIMULINK®) use the built-in function of the Rapp model for power amplifier analysis and the derived equivalent Rapp model parameter values can be easily used in these simulators by simple substitution to study and analyze millimeter wave systems rather than developing an entire millimeter wave power amplifier simulation model.

1.3 Thesis Outline

The thesis is organized as follows:

Chapter 2 talks about the background of wireless communication and brief literature re-

view on different types of distortion in a wireless communication system. A special emphasis is given on power amplifier distortions produced in the transmitter, its causes and effects on the signals passing through it and the behavior. A detailed study on existing nonlinear behavioral models of power amplifiers, its properties and applications are discussed. The next part of this chapter discusses about the behavior of power amplifiers at millimeter wave range. Exclusive behavioral nonlinear models for power amplifiers at microwave and millimeter wave is discussed. Some of the existing compensation mechanisms for nonlinear distortions, its advantages and drawbacks are also discussed in this chapter followed by a brief information on device identification.

Chapter 3 talks about the details of the proposed model of a pilot signal based nonlinear distortion compensator for a Multiple-Input Multiple-Output Space-Time Block Code (MIMO-STBC) system modulated by QAM (Quadrature Amplitude Modulation) technique. Results from computer simulation show that the proposed method has a significant performance in terms of the bit error rate of the system. The effect of the proposed method when the power amplifier works at different parameter values is also discussed. Finally, the application of this technique for identification of the transmitter is explained along with an analysis of the proposed method's performance.

Chapter 4 talks about the analytical performance of a millimeter wave Orthogonal Frequency Division Multiplexing (OFDM) wireless communication system in presence of power amplifier nonlinear distortions. An analytical expression for the symbol error probability has been derived to evaluate the performance of a millimeter wave system theoretically in presence of power amplifier distortions, which can be used to avoid the cumbersome evaluation of the system performance through complex simulations. The results of the analytical expression is compared to the computer simulated communication system and found to match each other

and thus can be concluded that the analytical expression can be used to theoretically calculate the performance of millimeter wave systems. The equivalent Rapp model parameters for the modified Bessel-Fourier series model (used to model millimeter wave power amplifiers) has also been calculated.

Chapter 5 summarizes the discussions and results from previous chapters, draws the conclusion and talks about potential future work.

Chapter 2

Communication Systems Background and Literature Review

In this chapter, a background on the technical aspects of wireless communication and a literature survey report related to the thesis content has been discussed. The first section describes the wireless communication system followed by a brief description of the types of distortion present in these systems in the next section. With a special emphasis on power amplifier nonlinear distortions, the third section discusses the definition and causes of nonlinear distortions on communication systems. The fourth section talks about the effects of nonlinear distortions in communication systems and in the fifth section, a discussion on the mathematical models used to model the behavior of power amplifiers producing nonlinear distortions is given, followed by the section on the discussion of the behavior of power amplifier at millimeter wave range and its applicable mathematical models. The behavior of millimeter wave power amplifiers is different from their behavior at ultra high frequency (UHF), which the present communication systems use, due to various effects such as attenuation, delay, crosstalk etc. occuring due to the frequency of operation. Further, a discussion on the currently available techniques for nonlinear distortion compensation is given followed by the last section giving a brief overview about the meaning and process of device identification.

2.1 Wireless Communication Systems

Wireless communication is a process of transmitting data from one device to another without any physical connections between them. Wireless systems consist of a transmitter which generates and transmits a wireless message signal (electromagnetic wave), a wireless channel through which this message signal propagates, and a receiver which intercepts and processes this signal to retrieve the transmitted data. Transmission of data is done after a process called as modulation where certain characteristics of a wave is varied or 'modulated' depending on what data is transmitted. The modulated data is propagated to the wireless media through antennas. Conventional techniques use single carriers i.e. signal with only one frequency and/or a single antenna. With technology advancement, multi carrier (signal with different frequency components) and multiple antenna systems have been developed for efficient and reliable communication and handle large data traffic [2]. These techniques include the Orthogonal Frequency Division Multiplexing (OFDM), Multiple-Input Multiple-Output (MIMO) etc. An emphasis on the MIMO systems and OFDM systems is given in this section, as these systems have been considered and implemented in this thesis.

2.1.1 Multiple-Input Multiple-Output Systems

Multiple-Input Multiple-Output (MIMO) systems are wireless communication systems which have multiple transmit and receiving antennas. One of the key source of distortion which corrupt the signal is the channel which introduce fading, attenuation and scattering of the signal. In a conventional single antenna communication, the channel distortions led to degradation and loss of information in the signal. This aroused the need for better channel state information for efficient compensation of channel distortion for which the MIMO systems were developed [6].

MIMO systems were developed to get a better estimate of the channel information using multiple transmit and receive antennas and multiple streams of data with the help of suitable coding techniques like Almouti coding [7]. In a MIMO system with n_{tr} transmit antennas and n_r receive antennas, the data is transmitted through n_{tr} antennas and the signal from each antenna follows a different propagation path through the wireless channel. The receiver receives the signal through n_r antennas and decodes the data to recover the transmitted data. Each of the signals from n_{tr} antennas undergo channel fading depending on the path traversed by the signal. The receiver receives multiple streams of the transmitted signal from n_r receive antennas. Each of the received signal carry the channel state information of its traversed path. Hence, with the knowledge of the transmitted data and multiple copies of received data, a better channel state information is estimated through suitable signal processing which is used to compensate the distortion in the signal.

Mathematically, the received signal of a MIMO communication system is modeled as [7]

$$y = Hx + W \tag{2.1}$$

where y is the received symbol vector, H is the channel gain matrix, x is the transmitted symbol vector and W is the Additive White Gaussian Noise (AWGN).

In a MIMO system, the symbol at the jth receive antenna at time t is expressed as [7]

$$\tilde{r}^{j}_{\mathrm{NL}}(t) = \sum_{i=1}^{n_{tr}} \alpha_{i,j} s^{i}(t) + w^{j}(t) \tag{2.2}$$

where $\alpha_{i,j}$ is the path gain between the ith transmit and jth receive antenna, $s^{i}(t)$ is the transmitted pilot symbol from antenna i at time t.

MIMO systems are widely used in many communication systems like mobile telephony (3GPP and 3GPP2 standards), Wireless Local Area Network (WLAN) standards etc. It is combined with OFDM systems and used in applications like Long Term Evolution (LTE) systems etc. MIMO is also combined with multiple transceiver systems (called Multi-user systems) and used for better efficiency and communication security applications.

2.1.2 Orthogonal Frequency Division Multiplexing Systems

Orthogonal Frequency Division Multiplexing (OFDM) system is a method of encoding digital data in multiple carriers such that the carrier signals are orthogonal to each other as shown in Fig. 2.1. It is a wide-band communication scheme developed for higher data rates which uses a large number of closely spaced orthogonal sub-carrier signals to carry data on several parallel streams or channels [2] [8]. The greatest advantage of this method is the significant improvement in its bandwidth efficiency due to the orthogonal spacing of the sub-carriers.

An OFDM system is represented by [9]

$$x[n] = \begin{cases} \frac{1}{N} \sum_{m=0}^{N-1} X_m e^{\frac{j2\pi mn}{N}} & \text{for} - N_g \leq n \leq N-1 \\ 0 & \text{otherwise} \end{cases} \tag{2.3}$$

where n is time index, N is the Inverse Fast Fourier Transform (IFFT) length of the OFDM system, N_g is the guard interval length, X_m is the complex data symbol in frequency domain in the mth subcarrier.

OFDM systems are also robust against channel distortions as they are viewed as slowly modulated narrow-band signals rather than a single wide-band signal. This, along with its

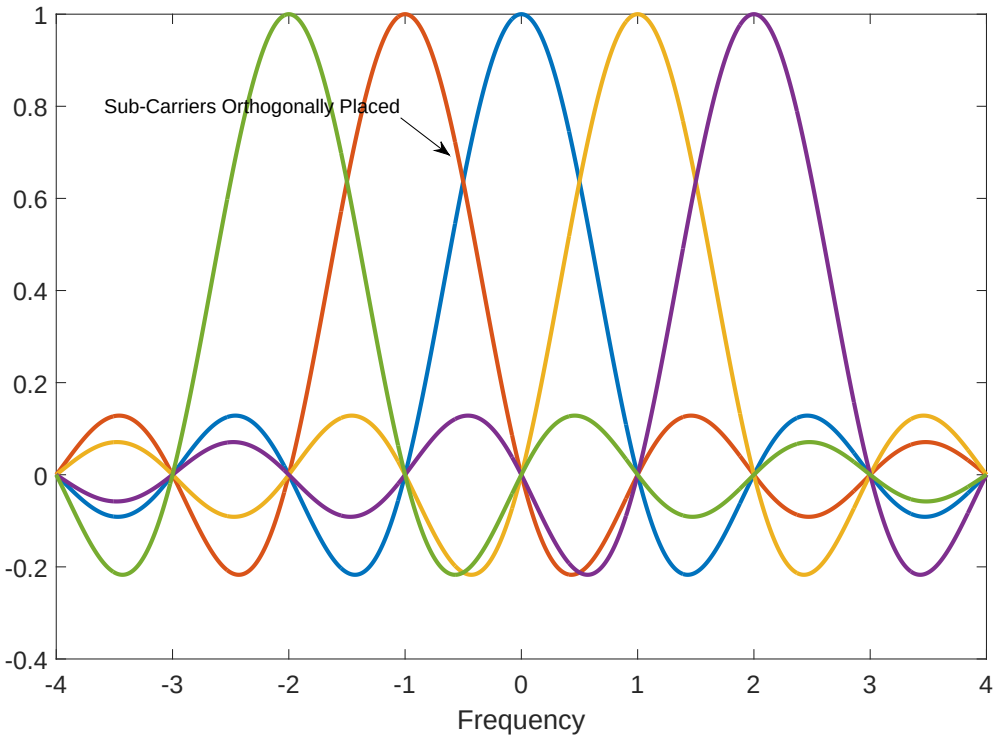

Figure 2.1: Orthogonally Spaced Sub-carriers in OFDM

implementation of Fast Fourier Transform (FFT) algorithm facilitates an easier implementation of equalizers at the receiver end. The use of guard interval in these systems also prevent inter-symbol interference, thus providing a higher quality of service. A summary of the merits and demerits of an OFDM system are as follows [10].

Merits

- High spectral efficiency due to orthogonal spacing of sub-carriers
- Easily adaptable to severe channel conditions without complex time-domain equalization
- Efficient implementation using Fast Fourier Transform

- Robust against inter symbol interference due to the presence of guard interval

Demerits

- Sensitive to Doppler shift
- High peak-to-average-power ratio (PAPR) which produce nonlinear distortions.

Due to the varied advantages of OFDM systems, these systems are widely employed in the present communication systems such as Wireless Local Area Network (WLAN), Digital Video Broadcasting (DVB), Digital Radio Systems and mobile networks like 3rd Generation Partnership Project (3GPP), 3GPP2 and Long Term Evolution (LTE) standards.

2.2 What Corrupts Data in Wireless Communication?

In wireless communication systems, the received signal will exactly not match the transmitted signal due to the introduction of distortions at various stages, right from the signal generation till it reaches the receiver. The primary sources of these distortions are from the transmitter device and the channel. Device distortions are produced due to the operating characteristics of the components used (such as a power amplifier [11]), or their imperfections during their manufacture (like IQ imbalance [12]) whereas the channel distortions are due to fading and multi-path signal propagation in wireless media [2] [13]. The various types of distortions caused due to circuit components include IQ imbalance, phase noise, carrier frequency offset, DC offset, sampling clock offset and power amplifier (PA) nonlinear distortions [2]. Though circuit distortions can be reduced by proper design of the components, it cannot be eliminated completely. Circuit distortions are mostly time invariant and specific to the characteristics of the transmitter circuit elements. The distortions due to the transmission channel are propagation delay, fading,

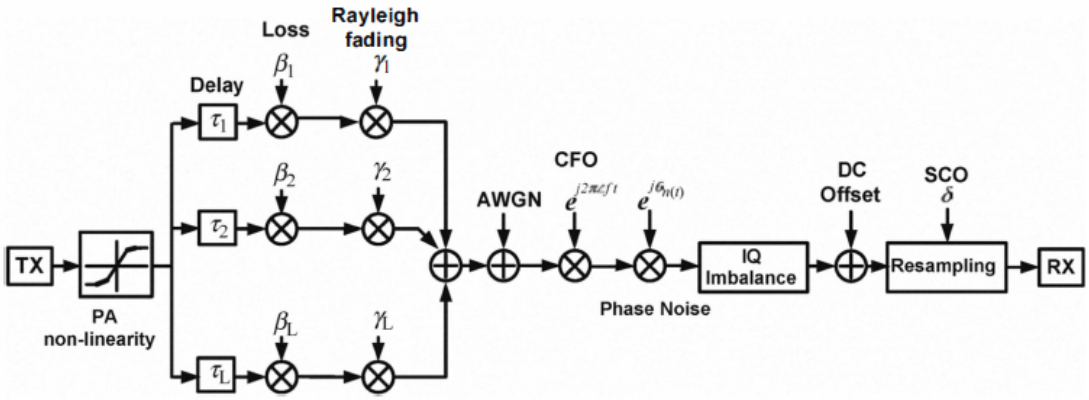

Figure 2.2: Various Distortions in a Communication System

scattering and multi-path propagation [2] [13]. These distortions are generally time variant due to the time varying nature of the channel and hence needs to be tracked on time-to-time basis. Fig. 2.2 shows the various types of distortions in a communication system [2].

Due to the addition of distortions in the transmitted signal, the received signal has to be processed to recover the original data from the distorted received signal. A component known as an equalizer, which is a filter, equalizes (removes) these distortions based on the equalizer weights set in the filter [2]. In almost all cases, a pilot signal based compensation is employed where a known signal is sent to estimate the time varying distortions. An adaptive equalizer equalizes the distorted signal at the receiver by adapting its weights, from the information of the distortions estimated periodically from the pilot signal. Most commonly used equalization techniques use the Least Mean Square (LMS), Normalized Least Mean Square (NLMS) and Recursive Least Square (RLS) algorithms to adapt the weights based on the information of the received pilot signal [14]. Equalization techniques are mostly implemented in the frequency domain, specially in OFDM systems, for easier processing though time-domain equalization

techniques are also proposed in literature [13] [15].

Generally, the equalizers employed are designed for compensating linear distortions and hence do not compensate nonlinear distortions effectively. Hence, for nonlinear distortions like the distortion produced by the power amplifier, current systems implement techniques at the transmitter end by operating the power amplifiers at levels such that no or minimal nonlinear distortions are introduced into the system, sometimes compromising the efficiency of the amplifiers. This is a trade-off between the efficiency and nonlinear distortion in the system; higher the efficiency of operation, more prone the signal to distortion. Thus, there is a need for receiver end compensation techniques in order to have a relatively better operating efficiency and less data corruption due to the distortions produced. Research work on receiver side compensation for these distortions have been proposed in literature [3] [16] [17] [18] [19].

2.3 Nonlinear Distortion: Definition and Causes

Nonlinear distortions are distortions produced in the signal due to certain nonlinear operation of transmitter components; Power amplifier (PA) is one of the main component of nonlinear distortion in transmitters as a virtue of its nonlinear operation due to saturation [11]. Power amplifier is a device which increases the power of the transmitted signal. Ideally power amplifiers increase the strength of the signal proportional to its gain but practical power amplifiers saturate beyond a certain value of power due to their limited operation range. This leads to clipping or distortions in the signal. In the frequency domain, the clipping of signals is represented as the production of additional frequency components called sidebands, which are undesirable as these sidebands interfere with adjacent communication signals thus impairing the information in those adjacent signals. Having sidebands is an offense and are strictly monitored by cellular

regulators using the concept of transmit spectrum mask [20].

Operating power amplifiers with high input back-off, thus forcing it to operate in the linear region is a solution to prevent nonlinear distortions, but at the cost of low efficiencies, whereas operating them in lower input back-off have high efficiencies but distorts the signal [3] [16]. For a better efficiency, the gain of the amplifier should be high enough, and at the same time should not clip/distort the signal, which is a trade-off. Thus, power amplifiers are operated at an operating point near saturation levels, so that the signal undergoes maximum possible amplification and minimum possible distortion to get an optimal performance. The various regions of operation of a power amplifier is shown in Fig. 2.3. This level of operation of the power amplifier still inevitably introduces some amount of distortions in all communication systems which need to be compensated. This thesis focuses on this aspect of the wireless communication system.

In order to compensate the nonlinear distortions at the receiver end, it is necessary to study the effect of nonlinear distortions in a wireless communication system through mathematical models. A signal has frequency, amplitude and phase, which get effected by nonlinear distortions. For multi carrier signals, nonlinear distortions effects on a signal are defined by two kinds; amplitude distortion and phase distortion [21]. These distortions can be either frequency dependent or independent. The amplitude distortions are defined by the AM-AM (Amplitude Modulation - Amplitude Modulation) conversion and phase distortions by AM-PM (Amplitude Modulation - Phase Modulation) conversion of the signal [21]. In AM-AM distortion, the amplitude of the output signal of the power amplifier is nonlinearly distorted (clipped) with respect to the amplitude of the input signal and the AM-PM distortion is the distortions in the phase of the output signal of the power amplifier with respect to the input signal [21]. AM-AM distortion happens due to the operating characteristics of the power amplifier because the

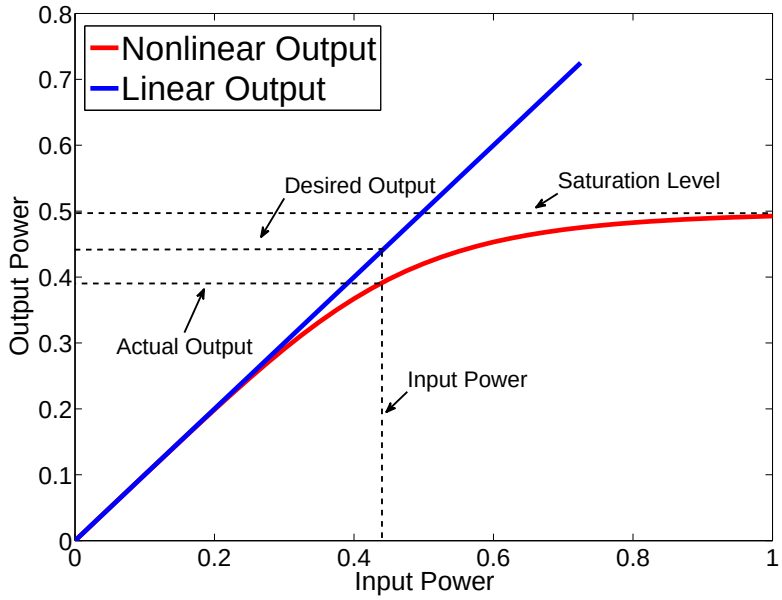

(a) Output Characteristics of Power Amplifier-Ideal vs. Practical

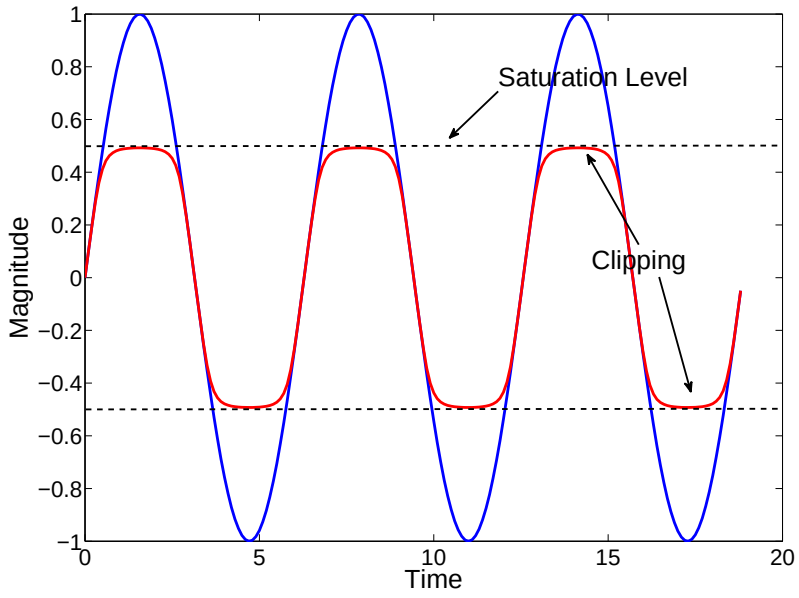

(b) Clipping Effect on sine wave due to Saturation of Power Amplifiers

Figure 2.3: Power Amplifier Operation Regions and Effects

power amplifier saturates beyond a certain level of input power and AM-PM distortion occurs due to the reactive effects of components such as transistors of the power amplifier circuit. At a given temperature, the power amplifier distortions do not vary [11]. Thus, power amplifier distortions can be considered as fairly static distortions [3].

2.4 Effects of Nonlinear Distortions

The noticeable effect due to PA nonlinear distortion is the clipping of signals in the time domain and compression of signal constellation due to this. Representing in the frequency domain, it leads to production of additional frequency components.

2.4.1 Compression of Signal Constellation

Wireless Communication involves a process called modulation; modulated signals are represented on a complex plane termed as signal constellation or constellation diagrams, with its in-phase (I) and quadrature (Q) components as shown in 2.4. Frequency independent modulation schemes such as Phase Shift Keying (PSK), Amplitude Shift Keying (ASK) and Quadrature Amplitude Modulation (QAM) are represented on constellation diagrams. Fig. 2.4a and Fig. 2.5a represents the constellation diagram for a 16-QAM and 16-PSK. The PSK and QAM has been considered here since these schemes are widely adopted in OFDM systems.

Nonlinear distortions lead to 'compression' of the regular constellation diagram at the output of the power amplifier. This means the magnitude of the constellation points 'compress' or gets moved towards the origin leading to distorted carrier wave. Fig. 2.4b and Fig. 2.5b shows the compressed constellation diagram when the modulated signal is subject to a Rapp model of nonlinearity (discussed later) [22]. Since, the Rapp model talks about only AM-AM distortion

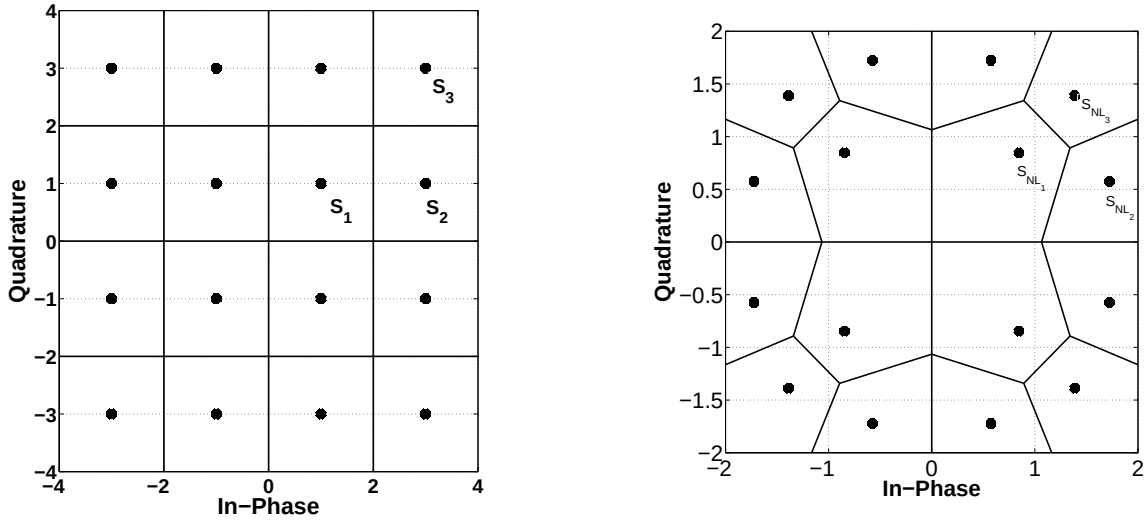

(a) Regular QAM

(b) Distorted QAM

Figure 2.4: Effect of PA Nonlinear Distortions on Constellations (along with decision regions)

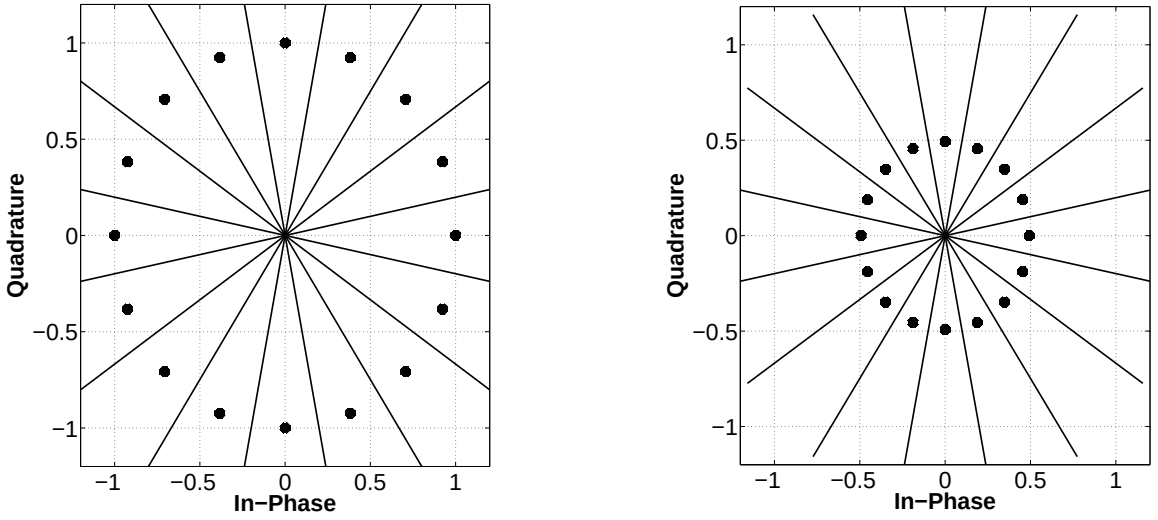

(a) Regular PSK

(b) Distorted PSK

Figure 2.5: Effect of PA Nonlinear Distortions on Constellations (along with decision regions)

and zero AM-PM distortion, the phase of the compressed points is the same as the original points as depicted in Fig. 2.4 and Fig. 2.5. It may be noticed from the figure that the effect of nonlinearity on the PSK constellation, though causes compression, still effects all the points of the constellation linearly. In other words, the decision region of the constellation points do not change. Hence, the process of demodulation is less complex and thus, the effect of nonlinearity on the performance of PSK system is negligible compared to a QAM.

The scenario is not the same for a QAM modulation. In QAM, the distortion undergone by each symbol varies nonlinearly i.e. symbols with different amplitudes undergo different levels of distortion. This is visible in the constellation diagram of Fig. 2.4 where the inner symbols are less/not compressed when compared to the outer symbols. The distortion leads to change in the decision region of the constellation points in a QAM [17]. In fact in nonlinear amplifiers modeled as a Rapp model with higher smoothness factors, the inner constellation points do not undergo any distortion. With the information of the nonlinear distortion, the error probability for the constellation with modified decision regions can be calculated using Craig's method [23].

Since the nonlinear distortions on QAM constellations has a greater effect on the performance of the wireless communication system, it becomes necessary to design nonlinear distortion compensators for QAM-modulated communication systems.

2.4.2 Effect on Power Spectrum

Power spectrum is the distribution of the power of the signal as a function of frequency. For single carrier systems, the appearance of harmonics due to nonlinear distortions is easier to analyze, since all frequency components other than that of the carrier signal, are distortions.

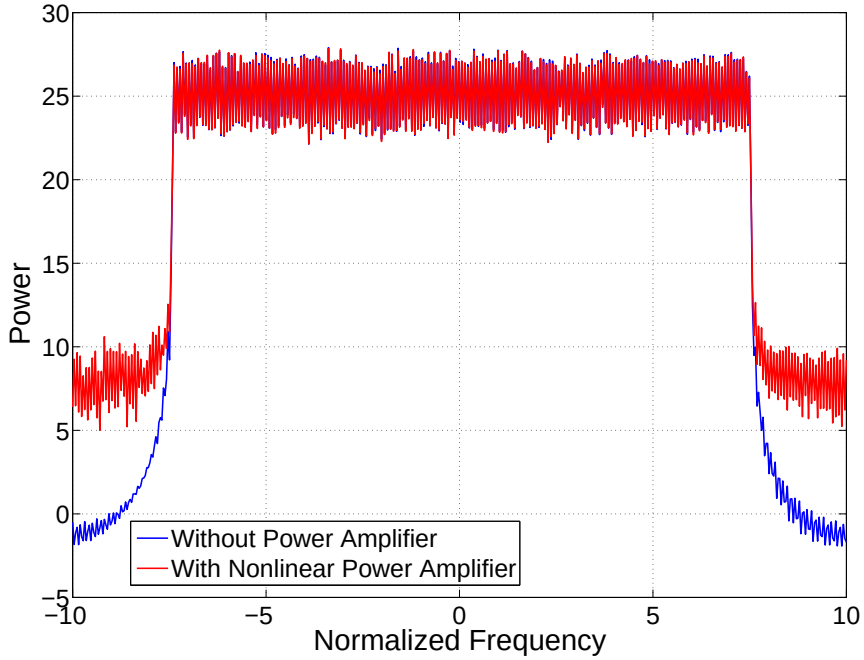

Figure 2.6: Power Spectral Density

But for multi carrier systems like Orthogonal Frequency Division Multiplexing (OFDM) signals, nonlinear distortions effects the power spectrum of the signal. When a signal containing a bandwidth of frequency components undergo nonlinear distortions, each frequency component in the transmitted range of frequencies of the signal produce harmonics. The frequency of these harmonics may correspond to another frequency component lying in the same bandwidth of the transmitted signal or may lie entirely outside the range. These harmonics which lie within the desired frequency band are called in-band distortions and the components outside this range are called out-of-band distortions or sidebands. The in-band distortions interfere with the desired frequency signals, attenuating or distorting the signals leading to degradation of symbol-error rate (SER) performance and capacity of the communication system [20]. The out-of-band distortions lead to spectrum broadening effects and interfere with the adjacent carriers.

The out-of-band distortions can be filtered using a band-pass filter but it is a challenging task to remove the in-band distortions, and these effect the SER performance of the communication system. Fig. 2.6 shows the power spectral density (PSD) of a multicarrier signal undergoing nonlinear distortion. The blue curve depicts the PSD of the original signal and the red curve depicts the PSD of the signal after undergoing nonlinear distortions. The figure clearly shows the appearance of side-bands, that is the frequency components outside the desired frequency range.

2.5 Behavioral Models of Nonlinear Power Amplifiers

The behavior of power amplifiers are represented mathematically using behavioral models for the purpose of analysis and simulation. The various power amplifier nonlinear distortion behavioral models are discussed below [24].

2.5.1 Polynomial Model

The polynomial model is a generic model used to define the nonlinearity of power amplifiers. Since nonlinear systems are expressed in the form of polynomials of increasing degree, power amplifier nonlinearity was described using this model. The polynomial model is given by [9] [25]

$$g[y(t)] = \sum_{d=1}^{D} a_{2d-1} x(t)|x(t)|^{2(d-1)} \tag{2.4}$$

where d is the order of the power amplifier nonlinearity, α is the power gain for order d, $y(t)$ is the output of the power amplifier for the input $x(t)$ in time domain. The order of the model defines the severity of nonlinearity; higher the order, the power amplifier is operated in a highly

nonlinear or saturation region.

In communication systems, power amplifiers are operated close to saturation levels and not in deep saturation to get optimum efficiency. This level of nonlinearity is the 'weakly' nonlinear distortion region and is best modeled with a third order ($2d - 1 = 3$ in equation 2.4) nonlinear polynomial for study purposes as the effect of higher order nonlinearities are negligible [9].

2.5.2 Saleh Model

With the intention of developing a better model to study nonlinear properties of power amplifiers, A A M Saleh defined a mathematical model in 1981 which is popularly called the Saleh Model [21]. This model introduced the concept of AM-AM and AM-PM nonlinear distortion and is extensively used to model Travelling Wave Tube Amplifiers (TWTA). The AM-AM distortion $g[y(t)]$ and AM-PM distortion $\phi[y(t)]$ for Saleh model is defined by

$$g[y(t)] = \frac{\alpha_a x(t)}{(1 + \beta_a x(t)^2)} \tag{2.5}$$

$$\phi[y(t)] = \frac{\alpha_\phi x(t)^2}{(1 + \beta_\phi x(t)^2)} \tag{2.6}$$

where $g[y(t)]$ and $\phi[y(t)]$ are the AM-AM output magnitude and AM-PM output phase of the signal with power amplifier distortion, α_a and β_a are the Saleh parameters for AM-AM distortion, α_ϕ and β_ϕ are the Saleh parameters for AM-PM distortion, $x(t)$ is the input signal envelope to the power amplifier.

The transfer characteristics of the Saleh model is as shown in Fig. 2.7 [26]. The Saleh model is a frequency dependent model i.e. its parameter values are different depending on the

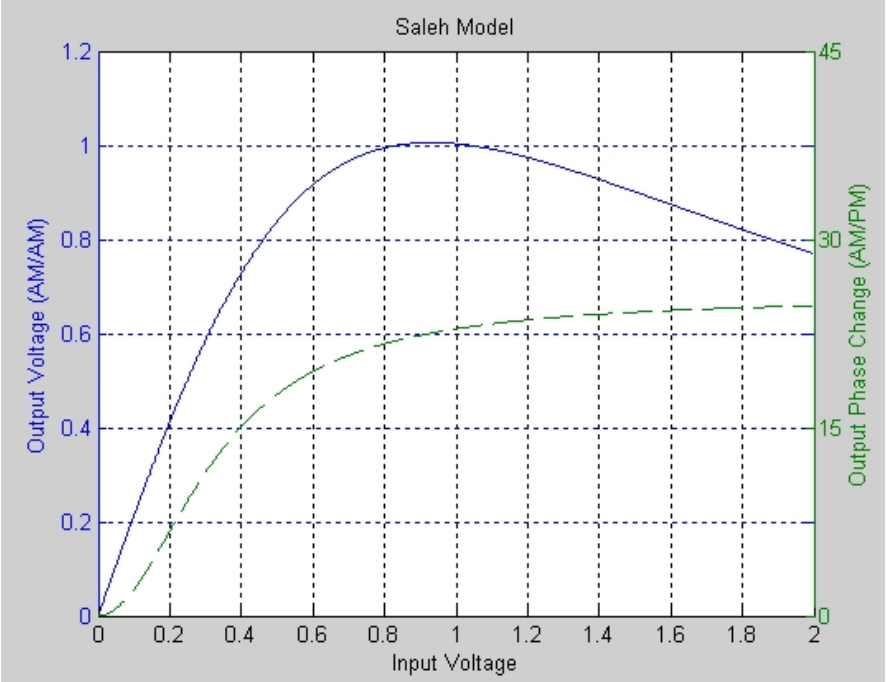

Figure 2.7: Output Characteristics of Saleh Model

frequency at which the power amplifier operates. Transmitters employing the TWTA amplifiers use this behavioral model for their study purposes and one of the most important application of this amplifier model in wireless communication is in satellite communications.

2.5.3 Modified Saleh Model

In 2009, a new model was developed to overcome certain weaknesses shown by the Saleh model and was called the modified Saleh model [27]. This model proposed a 6-parameter model to overcome the failure of the conventional Saleh model when the denominators of equation 2.5 and equation 2.6 equaled to zero. An additive term ϵ was introduced to the Saleh model which addressed this issue. The generic form proposed for the modified Saleh model is

given by [27]

$$f(x) = \frac{\alpha x^{\eta}}{(1+\beta x^{\gamma})^{\nu}} - \epsilon \tag{2.7}$$

Applying this proposed model and with some simplification [27], the AM-AM and AM-PM distortion due to the power amplifier considering the modified Saleh model is given by

$$\begin{aligned} g[y(t)] &= x(t).\frac{\alpha_a}{\sqrt{(1+\beta_a x(t)^3)}} \\ \phi[y(t)] &= x(t).\frac{\alpha_\phi}{\sqrt[3]{(1+x(t)^4)}} - \epsilon \end{aligned} \tag{2.8}$$

where $x(t)$ is the input of the signal, $g[y(t)]$ is the output magnitude of the signal, $\phi[y(t)]$ is the output phase of the signal, α_a and β_a are Saleh parameters for AM-AM distortion, α_ϕ and β_ϕ are the Saleh parameters for AM-PM distortion and ϵ is the newly introduced parameter to overcome the limitations of the traditional Saleh model.

For the AM-AM distortion, the value of the denominator in the traditional Saleh model cannot be zero and hence, ϵ is considered as zero [27].

2.5.4 Rapp Model

With the development of semiconductor technology, most power amplifiers employed today are solid state power amplifiers (SSPA). The nonlinear behavior of SSPA power amplifiers is slightly different from the TWTA models. In 1991, when solid state devices started becoming popular, Christopher Rapp developed another mathematical model to study the behavior of solid state power amplifiers defined by equation 2.9 [22]. This model was termed the Rapp model and is the most commonly used model of power amplifiers.

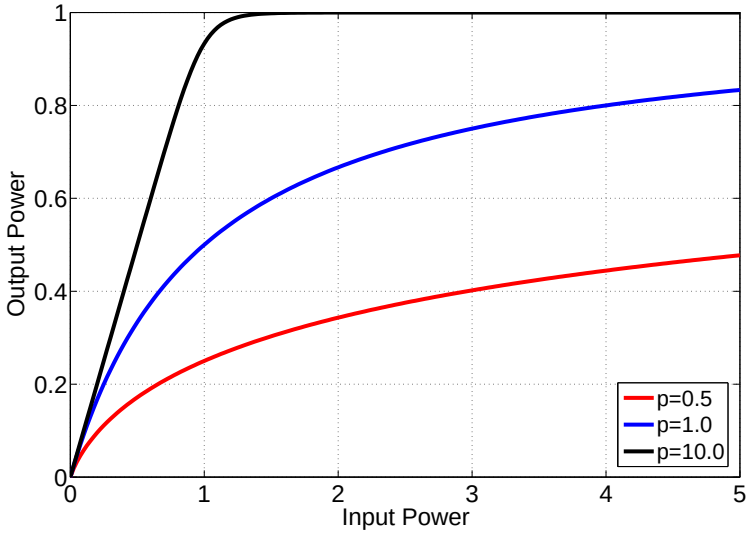

Figure 2.8: Output Characteristics of a Rapp Model

The Rapp model is defined using three parameters namely the small signal linear gain parameter A, saturation level parameter of the power amplifier x_0 and smoothness factor p. The AM-AM distortion $g[y(t)]$ and AM-PM distortion $\phi[y(t)]$ for Rapp model is defined by equation 2.9 [22]. The output characteristics for a Rapp model is as shown in Fig. 2.8.

$$g[y(t)] = x(t)\frac{A}{\left[1+\left(\frac{Ax(t)}{x_0}\right)^{2p}\right]^{\frac{1}{2p}}} \qquad (2.9)$$

$$\phi[y(t)] = 0$$

where $g[y(t)]$ is the output magnitude of the signal, $\phi[y(t)]$ is the output phase change of the signal.

The Rapp model clearly defines the saturation characteristic of power amplifiers, as evident from Fig. 2.4 and hence is the most extensively used power amplifier model to study SSPA distortions [3], [16], [17], [18], [19], [28].

2.5.5 Soft-Envelope Limiter Model

A soft envelope limiter model is used to model an ideal power amplifier which is described by the relation given in equation 2.10 between the input and output [17]

$$g[y(t)] = \begin{cases} Ax(t), & x(t) \leq x_0 \\ x_0, & x(t) > x_0 \end{cases} \tag{2.10}$$

where $g[y(t)]$ is the magnitude of the envelope of the output signal, A is the small signal gain of the power amplifier, $x(t)$ is the envelope of input signal, x_0 is the saturation level.

This model is defined by a sharp change in output magnitude at saturation levels i.e its value is proportional to the input until saturation and all values at and beyond saturation level is equal to the saturation level. This model is seldom used since practical power amplifiers show gradual change in its output characteristics as shown in Fig. 2.3 rather than sharp changes at the saturation point (P_{sat} in Fig. 2.3). As a matter of fact, the soft envelope limiter model is a particular case of the Rapp model with its smoothness factor p in equation 2.9 as infinity [29].

2.6 Behavioral Models of Millimeter Wave Power Amplifiers

The behavior of power amplifiers when operated by millimeter wave signals is different from its behavior at lower frequencies. Super High Frequency or SHF signals (Millimeter waves) undergo effects like delay, attenuation, dispersion etc. as they encounter parasitic effects of the circuit components (capacitors) produced at the junctions of the transistor used in the power amplifier [4]. Capacitances are energy storing elements and produce memory effects [30]. The

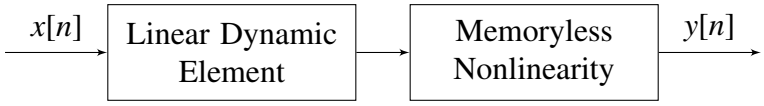

Figure 2.9: Wiener Model of Power Amplifier with Memory

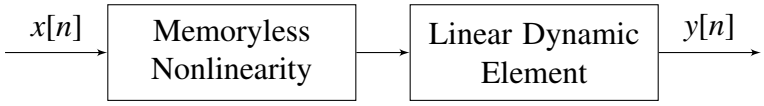

Figure 2.10: Hammerstein Model of Power Amplifier with Memory

voltage equation of a linear capacitance is given by [30],

$$v_C(t) = \frac{1}{C}\int_{-\infty}^{t} i(t)dt \tag{2.11}$$

where $v_C(t)$ is the output voltage at time t, C is the capacitance and $i(t)$ is the current at time t.

It can be seen clearly from this equation that the voltage at time instant t is dependent on the previous values of currents (integration over time from -∞ to t) which is why capacitances are considered as memory introducing circuit elements [30]. Due to the capacitive effects in power amplifiers at high frequencies, they are defined using memory models.

Mathematical models to depict memory are represented using an FIR filter since the current output of a FIR filter is a combination of present and past inputs. This closely resembles the capacitance effect of equation 2.11. Thus, in the digital domain, where the signal is sampled at time instants 'n', the output of an FIR filter having 'N' taps, for an input x[n] is written as

$$y[n] = \sum_{l=0}^{N-1} h[l]x[n-l] \tag{2.12}$$

where $y[n]$ is the output at time instant n, $h[l]$ is the co-efficient of lth tap of the 'N' tap filter.

Memory models for power amplifiers for millimeter waves are considered by including

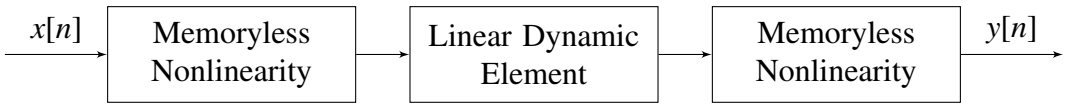

Figure 2.11: Wiener-Hammerstein Model of Power Amplifier with Memory

a combination of a linear dynamic element and a nonlinear component. Accordingly, many models such as the memory polynomial model [9], Wiener model, Hammerstein model and the Wiener-Hammerstein model [31] have been discussed in the literature. The Wiener model consists of a linear dynamic memory element followed by a memoryless nonlinear block to model the power amplifier characteristics. The Hammerstein model is the reverse of this combination and the Wiener-Hammerstein model is a cascade combination of the two models. Fig. 2.9, Fig. 2.10 and Fig. 2.11 show the Wiener, Hammerstein and Wiener-Hammerstein models for power amplifiers respectively. Further, to study power amplifiers at microwave with high memory effects, the general models used are the nonlinear dynamic feedback model and the nonlinear dynamic cascade model shown in Fig. 2.12 and Fig. 2.13 respectively.

2.6.1 Nonlinear Dynamic Feedback Model

The nonlinear dynamic feedback model of memory power amplifier for microwaves is shown in Fig. 2.12 [32]. It consists of a combination of the Wiener-Hammerstein model with a linear feedback filter across the nonlinear block. In the frequency domain, the forward filters are denoted by $H(\omega)$ and $O(\omega)$ and the feedback filter is denoted by $F(\omega)$ as shown in Fig. 2.12. This model is considered to study the strong memory effects arising due to the reactive components of the power amplifier. The memory component is modeled using the FIR filter and the nonlinear component is modeled by the polynomial model.

Considering this polynomial nonlinear model, the transfer characteristic of the power am-

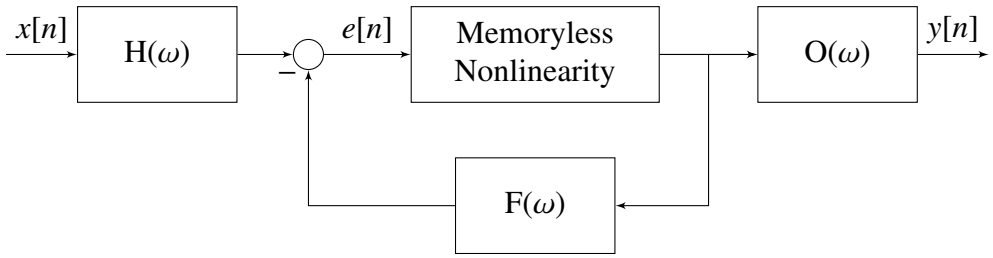

Figure 2.12: PA Nonlinear Dynamic Feedback Model

plifier with nonlinear distortions can be written as [32]

$$S_1(\omega) = H(\omega)\frac{a_1}{D(\omega)}O(\omega)$$

$$\begin{aligned} S_3(\omega_1,\omega_2,\omega_3) = {} & \frac{H(\omega_1)H(\omega_2)H(\omega_3)O(\omega_1+\omega_2+\omega_3)}{D(\omega_1)D(\omega_2)D(\omega_3)D(\omega_1+\omega_2+\omega_3)} \\ & .\left[a_3+\frac{2}{3}a_2^2\left(\frac{F(\omega_1+\omega_2)}{D(\omega_1+\omega_2)}+\frac{F(\omega_1+\omega_3)}{D(\omega_1+\omega_3)}+\frac{F(\omega_2+\omega_3)}{D(\omega_2+\omega_3)}\right)\right] \end{aligned} \tag{2.13}$$

where $D(\omega) = 1 - a_1F(\omega)$ which is the loop gain of the feedback path, $S_1(\omega)$ is the linear transfer function, $S_3(\omega_1,\omega_2,\omega_3)$ is the nonlinear transfer function and $H(\omega)$, $O(\omega)$ and $F(\omega)$ are filters to denote the memory effects for the memoryless nonlinear block in Fig. 2.12. The nonlinearity considered here is defined by a polynomial model as $a_1e[n] + a_2e[n]^2 + a_3e[n]^3$.

2.6.2 Nonlinear Dynamic Cascade Model

The nonlinear dynamic cascade model of memory power amplifier for microwaves is shown in Fig. 2.13 [30]. This model uses a cascade combination of Wiener-Hammerstein models. It consists of a combination of two nonlinearities with a linear filter in between. The filters in the forward path are denoted as $H(\omega)$, $F(\omega)$ and $O(\omega)$ in the frequency domain and the transfer

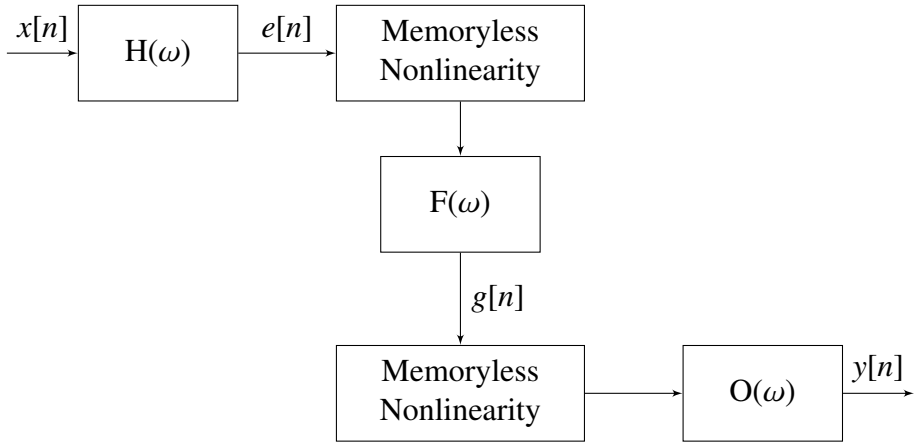

Figure 2.13: PA Nonlinear Dynamic Cascade Model with Memory

characteristic for the power amplifier model is given by [30]

$$
\begin{aligned}
S_1(\omega) &= H(\omega)a_1F(\omega)b_1O(\omega) \\
S_3(\omega_1,\omega_2,\omega_3) &= H(\omega_1)H(\omega_2)H(\omega_3)O(\omega_1+\omega_2+\omega_3) \\
&\quad .\Big\{a_3F(\omega_1+\omega_2+\omega_3)b_1+ \\
&\quad \frac{2}{3}a_1a_2\Big[F(\omega_3)F(\omega_1+\omega_2)+F(\omega_2)F(\omega_1+\omega_3)+ \\
&\quad F(\omega_1)F(\omega_3+\omega_2)\Big]b_2+a_1^3F(\omega_1)F(\omega_2)F(\omega_3)b_3\Big\}
\end{aligned}
\tag{2.14}
$$

where $S_1(\omega)$ is the linear transfer function, $S_3(\omega_1,\omega_2,\omega_3)$ is the nonlinear transfer function and $H(\omega)$, $F(\omega)$ and $O(\omega)$ are filters to denote the memory effects for the memoryless nonlinear block in Fig. 2.13. The nonlinearity considered here is defined by a polynomial model as $a_1e[n]+a_2e[n]^2+a_3e[n]^3$.

Thus, it is generalized that the dynamic cascade and feedback models are used to model microwave power amplifiers with strong memory effects [33]. Analysis of high memory effect

models is cumbersome which aroused a need to develop an equivalent memoryless model considering all the memory effects and studies in this direction are being made [34].

2.6.3 Bessel Fourier Series Model

A model to explain the nonlinear characteristics of the power amplifier was introduced, called the Bessel-Fourier series model, given by [34] [35] [36]

$$g[y(t)] = \sum_{p=1}^{P} b_p J_1\left(\frac{2\pi}{\gamma D} p x(t)\right) \tag{2.15}$$

where $g[y(t)]$ is the output signal with AM-AM distortion, $x(t)$ is the input, b_p is the pth coefficient of the Fourier series approximation, $J_1(.)$ is the Bessel function, D and γ are the dynamic range and dynamic range ratio parameter for the model [37].

Studies on choosing the right parameters for this model were carried out [35]. Due to inaccuracies and discrepancies, clarifications regarding the choice of right parameters were studied [38] [39]. Finally it is shown that certain modifications in this model led to higher accuracy of modeling of millimeter wave systems and was termed the modified Bessel-Fourier series model [37].

2.6.4 Modified Bessel Fourier Series Model

To overcome some of the drawbacks of the Bessel Fourier series model for power amplifiers, the modified Bessel-Fourier Series model was developed in 2013 by O'droma M and Lei Yim-

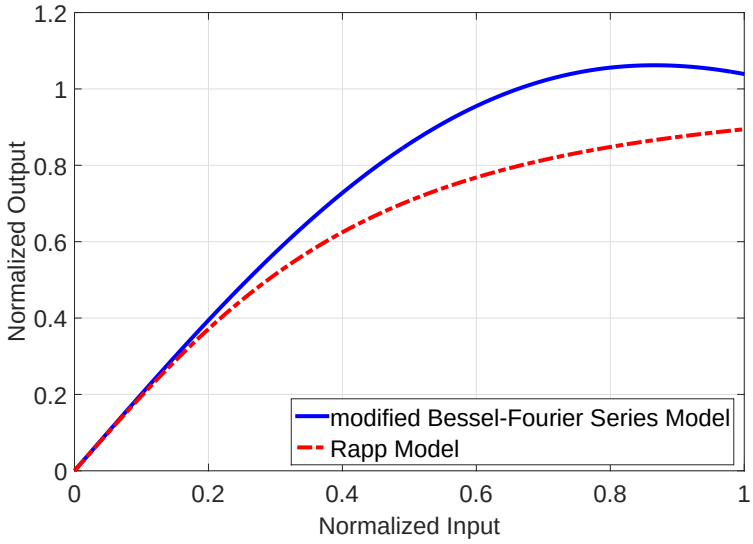

Figure 2.14: Output Characteristics of a modified Bessel-Fourier Series Model for PA

ing, and is defined as [37]

$$g[y(t)] = \sum_{p=1}^{P} b_{(2p-1)} J_1\left(\frac{2\pi}{\gamma D}(2p-1)x(t)\right) \tag{2.16}$$

where $g[y(t)]$ is the nonlinearly distorted signal, P is the Bessel-Fourier series order, $b_{(2p-1)}$ is the $(2p-1)$th coefficient of the Fourier series approximation, $J_1(.)$ is the Bessel function, D and γ are the dynamic range and dynamic range ratio parameter for the model [37].

With the need to develop an equivalent memoryless model for millimeter wave power amplifiers for simpler analysis and modeling, studies on the characteristics of these power amplifiers were carried out in literature [34]. With the help of actual measurements of a Laterally Diffused Metal Oxide Semiconductor (LDMOS) power amplifier, it has been established that the modified Bessel-Fourier series model is the most suited power amplifier model for millimeter wave amplifiers [34]. The order of the modified Bessel-Fourier series to model a power

amplifier at millimeter wave range is $P = 3, 10$ and $\gamma = 3.8, 4.2$ respectively in (2.16) [34] [37]. The optimum value for the term α=$2\pi/\gamma D$ in equation 2.16 is 0.6 [40]. The output characteristics of the power amplifier model for millimeter waves using the modified Bessel-Fourier series model is shown in Fig. 2.14. This figure also compares the millimeter wave power amplifier characteristics with the output characteristics of Rapp model (with parameters $A = 2$, $p = 1$ and $x_0 = 1$).

2.7 Nonlinear Distortion Compensation Techniques

The effect of nonlinear distortion leads to clipping of signal in the time domain or the growth of additional frequency components as sidebands in frequency domain. The obvious compensation which needs to be done is to filter out the additional frequency components. The simplest method to do this would be the use of a band pass filter which is a device that allows signals of a particular range of frequencies through it filtering out the other frequency components in the signal. Though the method appears simple, the drawback of this compensation mechanism is that for narrow band or single carrier signals, the design of extremely narrow bandpass filter would be a challenge due to its higher order and unstable filter design [41]. For multicarrier signals, the design of bandpass filters may be easy due to their wideband operation and the out of band frequency components can be easily filtered out but the in-band distortions cannot be filtered out by the bandpass filter (Refer Fig. 2.6).

One of the most common method of nonlinear distortion compensation is the use of a predistorter at the transmitter end before the power amplifier [3]. A predistorter is a model defined by a generic complex function which implements the inverse of a defined power amplifier nonlinear model before the power amplifier segment of the transmitter [3]. Thus, the signal is

compensated for nonlinear distortions at the transmitter end even before signal transmission and hence, the receiver has to process for only the channel distortion. For power amplifiers having memory effects, predistorters for their nonlinear distortion compensation is proposed by the concept of look-up tables [42]. Though the predistortion method is an effective method of nonlinear distortion compensation, it involves additional signal processing at the transmitter end. Also, the predistortion method has a poor performance in low-IBO (Input Back Off) regions [3]. Hence, a receiver side nonlinear compensation is an assuring solution since the receiver already has signal processing blocks [16].

Many receiver side nonlinear compensation techniques have been proposed in literature [3] [16] [17] [18] [19] [43]. Nonlinear compensation can be done using hard decision rules and adaptive/iterative processes involving numerous Fast Fourier Transforms (FFT) and Inverse Fast Fourier Transform (IFFT) but causes intensive signal processing at the receiver [16] [18] [19] [43]. Though the methods are effective, they lead to higher order complexity at the receiver which may further effect the size and temperature aspects of the receiver design. The complexity further increases with larger number of received samples.

Alternative receiver side compensation techniques include the use of Sequential Monte Carlo (SMC) algorithm methods for nonlinear distortion compensation [3] [17]. This involves the estimation of transmitted data based on the received samples using SMC algorithms. SMC based compensation methods proposed in literature considers a MIMO system and derives a model for nonlinear compensation based on the probability distribution of power amplifier parameters at each of the transmitter antennas [17]. The received sample set of data from the pilot signal is used to estimate the distribution using SMC methods. These methods are efficient but intensive as they are iterative in nature, thus still involving complex processing at the receiver.

Nonetheless, there are compensation mechanisms being developed for power amplifier non-linear distortions but each method has its own drawback in terms of efficiency or the complexity of signal processing. There has always been a trade-off between complexity and efficiency in the designs involved.

2.8 Device Identification

'Device Identification' is a process of uniquely identifying a communication device using its distinctive feature(s). Devices are traditionally identified by some unique information that they hold such as a public identifier or a secret key. Besides by what they hold, devices can be identified by what they are, i.e., by some unique characteristics that they exhibit and that can be observed such as the operating system, drivers, clocks, radio circuitry, etc. [44]. It is proposed to use device dependent *radiometrics* as fingerprints to detect identity spoofing. *Radiometric* is a component of the radio signal such as amplitude, frequency, phase or any feature derived from those components. Each device creates a unique set of *radiometrics* in its emitted signal due to hardware variability such as in the antennas, power amplifiers, ADC, DAC, etc. [45]. These *radiometrics*, once produced in the signal, do not alter and thus provide a reliable means for identification. The device identification process involves verifying the identity of the device using one of these *radiometric*. Techniques that allow wireless devices to be identified by unique characteristics of their analog (radio) circuitry are referred to as physical-layer device identification.

Physical-layer device identification involves three entities; a wireless device, a device identification system, and an application system requesting the identification [44]. Physical-layer device identification systems aim at identifying (or verifying the identity of) devices based on

characteristics of devices that are observable from their communication at the physical layer i.e., physical-layer device identification systems acquire, process, store, and compare signals generated from devices during communications with the ultimate aim of identifying (or verifying) devices. Some of these observable characteristics are the IQ imbalance, power amplifier nonlinearities etc [45]. A physical-layer identification system has the tasks to acquire the identification signals (acquisition setup), extract features and obtain fingerprints from the identification signals (feature extraction module), and compare fingerprints (fingerprint matcher).

Physical-layer identification is one of the reliable method for device identification since the principle is based on a observable quantity of an actual hardware circuitry used in communication which is specific to that device. Hence, any other device trying to interpret as the original device can be easily identified since the characteristics of the hardware circuitry used in this device is completely different from the original one. This would mean the interpreting device should have a hardware with characteristics exactly similar to that of the original device which is highly improbable and thus can be an efficient mechanism of physical layer security. The physical layer device identification technique can also be combined with techniques in different layers for a collaborated approach for device identification.

2.9 Summary

In this chapter, the background information about the wireless communication system with an introduction of the MIMO and OFDM techniques has been given. Various sources of distortion in a typical wireless communication system were discussed with a special emphasis on the power amplifier nonlinear distortions. The effects of nonlinear distortion on the constellation diagram and the power spectral density was studied along with a literature survey of the

available power amplifier behavioral models at normal and high frequencies (memoryless and memory models), currently available compensation mechanisms for nonlinear power amplifier distortions and its advantages and disadvantages. This was followed by a brief understanding of 'Device Identification' and its process.

2.10 Conclusions

The following are the conclusions from this chapter.

- The effect of power amplifier nonlinear distortions is mostly severe in QAM systems due to changes in decision region of the symbols and hence, it is essential to develop compensation mechanisms for QAM communication systems (Fig. 2.4). Thus, QAM systems have been considered for the analyses in this thesis.

- From literature, is it established that the Rapp model is the best suited behavioral model for modeling the effect of power amplifier nonlinearity as it clearly depicts the saturation phenomenon of SSPAs [22]. Since most present day systems use SSPAs, analysis of power amplifiers has been done using the Rapp model in this thesis with the intention of application of the proposed methods for practical SSPAs.

- Power amplifier behavior in the millimeter wave range is different from the UHF range and it is established that the modified Bessel-Fourier series model is the suitable behavioral model to study and analyze power amplifiers in millimeter wave systems [34]. Hence this model has been considered for millimeter wave power amplifier analyses in this thesis.

- Physical layer device identification can be done based on the set of unique *radiometrics* produced by a component of the transmitter device. One of such an application of identification of transmitter device using these *radiometrics* has been considered in this thesis.

Chapter 3

Pilot Signal Based PA Distortion Compensation and Device Identification

3.1 Introduction

In wireless communication systems, distortions are compensated at the receiver end of the wireless communication system using methods with a primary focus on retrieving the original signal, irrespective of their source of distortion. In this chapter, a methodology to identify the sources of distortion separately, its compensation and application in a transmitter device identification process is proposed using a two-step pilot signal approach. The methodology of identifying the source of device distortion, which is time invariant and channel distortions, which is time variant, separately is intended to reduce the complexity of the distortion compensator as the parameters for the time invariant distortion compensation, once estimated need not be re-estimated again. In the two-step process in this proposed methodology, step one involves the estimation of the channel and the step two estimates the transmitter parameters which are used to compensate distortions and identify the device. The device identification process involves the comparison of the estimated RF transmitter device parameters with a validated set of parameters.

The proposed method is illustrated by implementing it on a MIMO-STBC (Multiple Input Multiple Output-Space Time Block Code) system modulated by a QAM (Quadrature Amplitude Modulation), considering the Power Amplifier (PA) distortions (which are specific to a transmitter) and the MIMO channel distortions (which changes with changing channel characteristics). Identifying the power amplifier distortion separately and using a static means of compensation with fixed parameters for these distortions reduces the signal processing complexity at the receiver. Results from computer simulation show that the proposed compensation method has a significantly good performance in terms of the bit error rate of the system and successfully identifies the transmitter device.

In the proposed method, a focus on identifying the power amplifier and channel distortion is based on the use of symbols in the pilot signal present at different positions of the constellation. The fact that the channel distortions impairs all the symbols of the constellation equally while the nonlinear distortion significantly effects only the outer symbols in the constellation in Solid State Power Amplifiers (SSPAs) makes it a key point to identify and estimate these sources of distortion separately. With this information, the received signal is first compensated for the channel by channel estimation and equalization technique, and the power amplifier distortions are compensated by a parameter estimation and implementing them in an inverse model at the receiver.

Power amplifiers create a unique set of radiometric information which cannot be altered post production [45]. This radiometric information of the power amplifier can be defined by behavioral models which are functions of certain parameters. In this project, the power amplifier parameters estimated during the two-step process containing this radiometric information is used to identify the transmitter device as they are device specific.

The chapter is organized as follows. Section 3.2 describes the system model considered,

Section 3.3 describes the compensation mechanism for the channel and power amplifier distortions along with the estimation of the amplifier parameters of the transmitter. Section 3.4 describes the transmitter identification methodology followed by section 3.5 giving the system implementation and simulation results. Section 3.6 describes the effectiveness of the nonlinear compensator for variation in parameter values of the power amplifier and Section 3.7 draws the summary of the proposed mechanism.

3.2 System Model

A discrete-time baseband model with QAM STBC encoded Multiple Input Multiple Output (MIMO) communication system with n_{tr} transmitting and n_r receiving antennas, subject to power amplifier nonlinear distortions and channel is considered as shown in Fig. 3.1. Before the data transmission, two kinds of pilot sequences are generated; X^{T1} for step one, consisting of only the inner symbols of the constellation s_{in} having lower magnitude, (Symbol kinds inside dotted box of Fig. 3.2 and Fig. 3.3), to estimate the channel state information as they are not affected significantly by power amplifier distortions and X^{T2} for step two, which contains the outer symbols of the constellation, s_{out} (Symbol kinds outside dotted box of Fig. 3.2 and Fig. 3.3), as these symbols have higher magnitude and are susceptible to power amplifier distortions due to clipping and can be used to extract the power amplifier parameters at the receiver. The number of symbols in the set of s_{in} and s_{out} depend on the number of points of QAM and hence, pilot signals are designed appropriately according to the QAM scheme used, mainly using symbols which undergo negligible distortions in X^{T1} and high distortion in X^{T2} due to the power amplifier. The pilot sequences X^{T1} and X^{T2} can be either transmitted in two stages or combined and transmitted in a single stage. A Rapp model [22] is considered

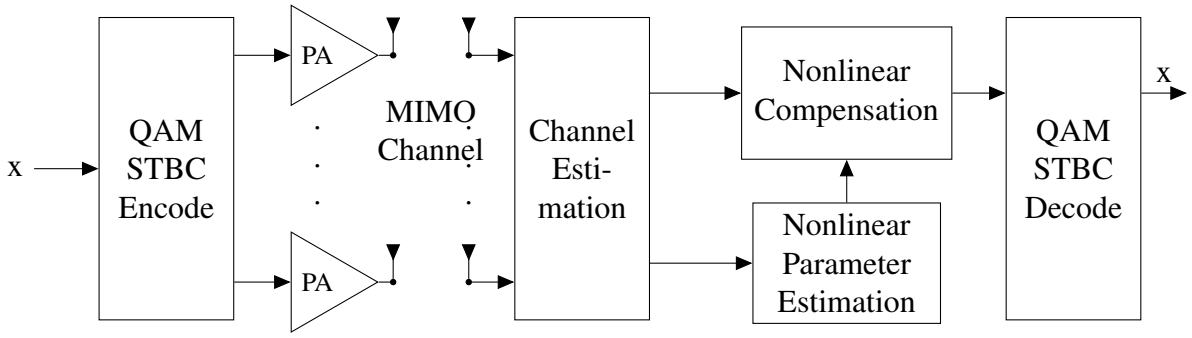

Figure 3.1: System Model for the Proposed Communication System

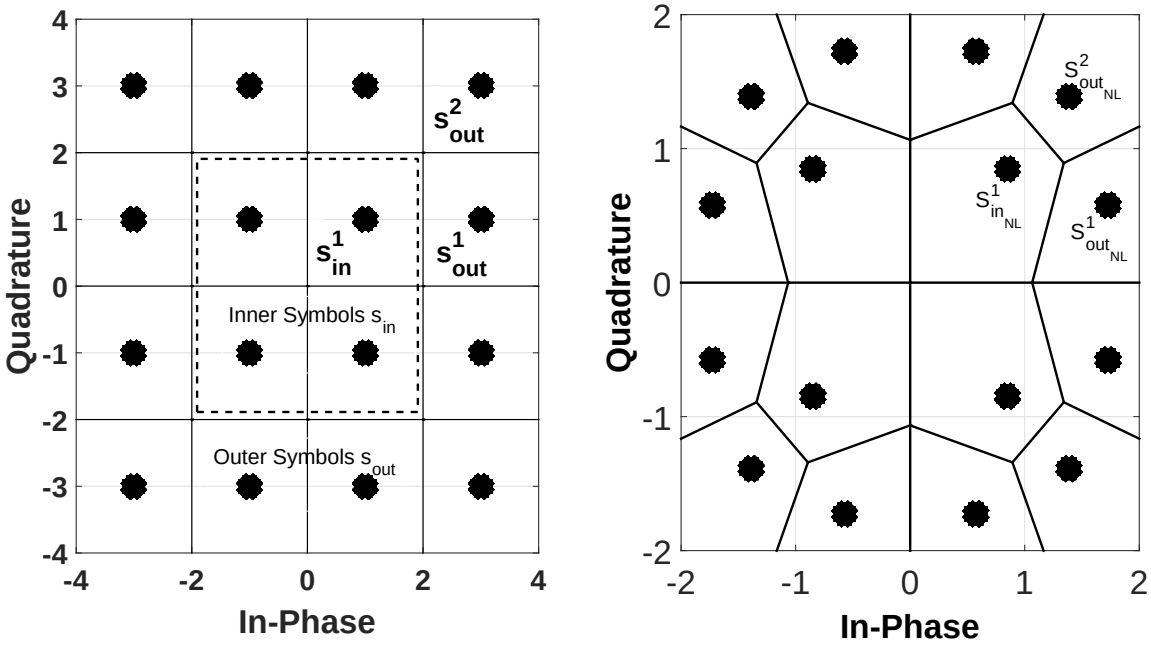

(a) Regular QAM

(b) Distorted QAM

Figure 3.2: Compression in 16-QAM Constellations (along with decision regions)

for power amplifier distortions as this model clearly depicts the clipping effects of the signal of higher magnitude and extensively used to model Solid State Power Amplifiers (SSPA) [3], [16].

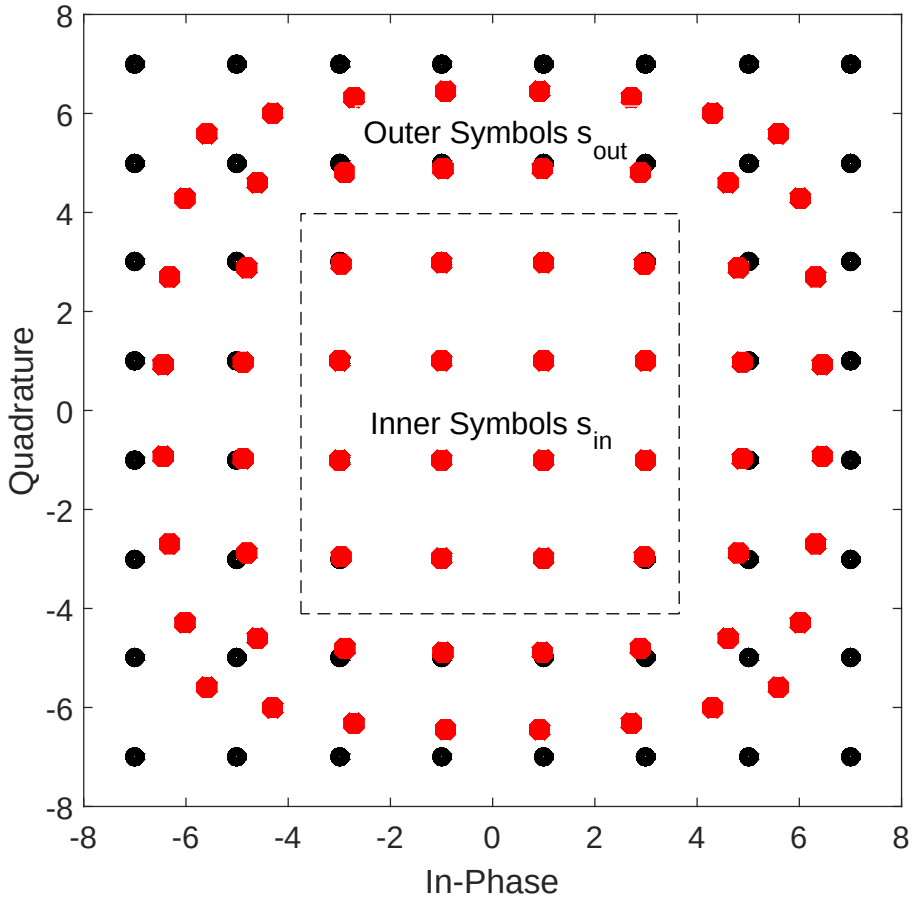

Figure 3.3: Compression in 64-QAM System

The modulated data vector considered, in its complex and polar form, is represented as

$$X = [x[1]\ x[2]\ x[3]\ ...\ x[T]]^{Tran} \tag{3.1}$$

$$X = [|x[1]|e^{j\theta_1}\ |x[2]|e^{j\theta_2}\ |x[3]|e^{j\theta_3}\ ...\ |x[T]|e^{j\theta_T}]^{Tran} \tag{3.2}$$

where $t = 1, 2, ..., T$ are the discreet time instants with total symbol duration of T, $|x[t]|$ represents magnitude of symbol $x[t]$ with its linear gain, θ_t represents the phase of the symbol and

Tran means the transpose.

When subjected to nonlinear distortions due to the power amplifier at baseband, each nonlinearly distorted symbol is given by [22]

$$\begin{aligned} |x_{\mathrm{NL}}[t]| &= \frac{|x[t]|}{\left[1 + (\frac{|x[t]|}{x_0})^{2p}\right]^{\frac{1}{2p}}} \\ &= |x[t]|.d[t] \end{aligned} \tag{3.3}$$

where

$$d[t] = \frac{1}{\left[1 + \left(\frac{|x[t]|}{x_0}\right)^{2p}\right]^{\frac{1}{2p}}} \tag{3.4}$$

is the power amplifier distortion factor by which the magnitude of the transmitted symbol is distorted, $|x[t]|$ is the magnitude of the amplified input signal (product of the linear gain A and the input signal has been considered here), x_0 is the output saturation level parameter and p is the smoothness factor of the power amplifier. Here, x_0 and p are power amplifier parameters which are specific to the transmitter device. Since the SSPA does not introduce phase distortion [22], the data vector in the polar form with nonlinear distortions is

$$\begin{aligned} X_{\mathrm{NL}} &= [|x_{\mathrm{NL}}[1]|e^{j\theta_1} \;\; |x_{\mathrm{NL}}[2]|e^{j\theta_2} \;\; ... \;\; |x_{\mathrm{NL}}[T]|e^{j\theta_T}]^{Tran} \\ &= [d[1]|x[1]|e^{j\theta_1} \;\; d[2]|x[2]|e^{j\theta_2} \;\; ... \;\; d[t]|x[T]|e^{j\theta_T}]^{Tran} \\ &= X \circ D \end{aligned} \tag{3.5}$$

where X is as given in equation 3.2, $D = [d_1 \;\; d_2 \;\; \ldots d_T]^{Tran}$ is the power amplifier distortion vector where each element is defined by equation 3.4 and $(X \circ D)$ is the hadamard product (el-

ement wise multiplication) of the power amplifier distortion term with the modulated symbol. In the complex form, it is written as

$$X_{\mathrm{NL}} = [x_{\mathrm{NL}}[1]\ \ x_{\mathrm{NL}}[2] \ldots x_{\mathrm{NL}}[T]]^{Tran} \tag{3.6}$$

where X_{NL} is a $T \times 1$ vector of transmitted symbols.

The signal containing power amplifier distortions passes through a MIMO wireless channel with n_{tr} transmit antennas and n_r receive antennas. Thus, the received matrix when the symbols are transmitted for a symbol duration T is [17]

$$Y = H\tilde{X}_{\mathrm{NL}} + W \tag{3.7}$$

where H is the $n_r \times n_{tr}$ channel gain matrix, Y is the $n_r \times T$ received signal matrix and $\tilde{X}_{\mathrm{NL}}$ is the $n_{tr} \times T$ transmitted symbol matrix of X_{NL} after STBC coding with power amplifier distortions, W is the $n_r \times T$ in-band Additive White Gaussian Noise (AWGN) matrix.

3.3 Compensation Mechanism

3.3.1 Channel Estimation and Equalization

To eliminate the channel distortions, an estimate of the channel $\hat{H}$ needs to be determined. The first step of the pilot signal performs this operation using X^{T1}. It is assumed that the channel distortions are constant for one time frame ($t = 1 \ldots T$) but varies from frame to frame. The pilot sequence X^{T1} of size $T_{T1} \times 1$ consisting of the inner symbols of the constellation (i.e.

$X^{\mathrm{T1}} \in \{s_{\mathrm{in}}\}$ of Fig. 3.2) undergo negligible power amplifier nonlinear distortions and the pilot signal vector at the power amplifier output will be $X_{\mathrm{NL}}^{\mathrm{T1}} \cong X^{\mathrm{T1}}$. When transmitted through the channel, the received signal is given by

$$Y^{\mathrm{T1}} = H\tilde{X}^{\mathrm{T1}} + W^{\mathrm{T1}} \tag{3.8}$$

where Y^{T1} is the $n_r \times T_{\mathrm{T1}}$ received pilot signal matrix at n_r antennas and $\tilde{X}^{\mathrm{T1}}$ is the $n_{tr} \times T_{\mathrm{T1}}$ transmitted pilot symbol matrix transmitted through n_{tr} antennas, W is the $n_r \times T_{T1}$ AWGN matrix and $T_{\mathrm{T1}}(< T)$ is the symbol duration for the pilot signal X^{T1}. It must be noted here that X^{T1} is the pilot vector while $\tilde{X}^{\mathrm{T1}}$ is the pilot signal matrix after STBC encoding.

Since X^{T1} is not significantly affected by the power amplifier nonlinearities, the received pilot signal Y^{T1} mainly contains the channel distortions. The unknown channel co-efficients H, denoted as $\hat{H}$ can be estimated using the least square estimate as [17]

$$\hat{H}_{\mathrm{LS}} = \arg\min_{\hat{H}} ||H\tilde{X}^{\mathrm{T1}} - Y^{\mathrm{T1}}||_F^2 \tag{3.9}$$

where $||.||_F$ is the Frobenius norm.

3.3.2 Nonlinear Distortion Estimation and Compensation

With the estimate of the channel obtained, step two of the proposed method to estimate power amplifier parameters is discussed in this section. An inverse Rapp model is considered at the receiver to compensate the power amplifier distortion which is derived from equation 3.3 and

is defined by, [3]

$$|x_n| = \frac{|x_{\mathrm{NL}_n}|}{\left[1 - \left(\frac{|x_{\mathrm{NL}n}|}{x_0}\right)^{2p}\right]^{\frac{1}{2p}}} \tag{3.10}$$

The application of this inverse model as a predistorter at the transmitter end to compensate power amplifier distortions exists and can be easily implemented as the parameters are known at the transmitter [3]. On similar lines, this model is implemented at the receiver end in this proposed method, which requires the estimation of the parameters p and x_0. It is considered that all power amplifiers in the MIMO transmitter exhibit same nonlinear behavior, which means they are defined by same values of parameters x_0 and p [17]. This assumption can be considered since all power amplifiers are connected to the same power source and will work identically.

To estimate these parameters, the second pilot signal vector X^{T2} of size $T_{\mathrm{T2}}\times 1$, consisting of the outer symbols of the constellation, s_{out} is used (Fig. 3.2 and 3.3), as these symbols undergo significant distortion due to power amplifier nonlinearities. For the case of 16-QAM, there are two outer symbols labeled as $\{s^1_{\mathrm{out}}, s^2_{\mathrm{out}}\}$ (Fig. 3.2) which are used in X^{T2}. Let their representation with power amplifier nonlinear distortion be $\{s^1_{\mathrm{out_{NL}}}, s^2_{\mathrm{out_{NL}}}\}$ respectively (Fig. 3.2). Since, it is required to estimate 2 parameters, two symbols are used in X^{T2} to solve for the parameters. After signal transmission, the representation of the received MIMO pilot signal X^{T2} containing the channel and nonlinear distortions in the matrix form is given by

$$Y^{\mathrm{T2}} = H\tilde{X}^{\mathrm{T2}}_{\mathrm{NL}} + W^{\mathrm{T2}} \tag{3.11}$$

where Y^{T2} is the $n_r \times T_{\mathrm{T2}}$ nonlinearly distorted received pilot signal with channel distortions

received through n_r antennas, $\tilde{X}_{\mathrm{NL}}^{\mathrm{T2}}$ is the $n_{tr} \times T_{\mathrm{T2}}$ transmitted pilot symbol matrix transmitted from n_{tr} antennas, W^{T2} is the $n_r \times T_{\mathrm{T2}}$ AWGN matrix and $T_{\mathrm{T2}}(< T)$ is the symbol duration for the pilot signal X^{T2}. Again it must be noted here that X^{T2} is the pilot vector while $\tilde{X}^{\mathrm{T2}}$ is the pilot signal matrix after STBC encoding.

In a MIMO system, from the received signal matrix, the symbol at the jth receive antenna at time t can be expressed as [7]

$$\tilde{r}_{\mathrm{NL}}^{j}(t) = \sum_{i=1}^{n_{tr}} \alpha_{i,j} s^{i}(t) + w^{j}(t) \tag{3.12}$$

where $\alpha_{i,j}$ is the path gain between the ith transmit and jth receive antenna, $s^{i}(t) \in \{s_{\mathrm{out_{NL}}}^{1}, s_{\mathrm{out_{NL}}}^{2}\}$ is the transmitted pilot symbol from antenna i at time t with nonlinear distortion information.

With the channel state information obtained from equation 3.8, the channel distortions in Y^{T2} are compensated and STBC decoded, and the pilot signal vector containing the nonlinear distortion and AWGN with symbols $\{\tilde{s}_{\mathrm{out_{NL}}}^{1}, \tilde{s}_{\mathrm{out_{NL}}}^{2}\}$ is obtained, where $\{\tilde{s}_{\mathrm{out_{NL}}}^{1}, \tilde{s}_{\mathrm{out_{NL}}}^{2}\}$ are received symbols corresponding to symbols $\{s_{\mathrm{out_{NL}}}^{1}, s_{\mathrm{out_{NL}}}^{2}\}$ respectively containing AWGN.

With AWGN the pilot symbols with power amplifier distortions, $\tilde{s}_{\mathrm{out_{NL}}}^{l} \sim \mathcal{N}(\hat{s}_{\mathrm{out_{NL}}}^{l}, \sigma_{NL}^{2})$. The maximum likelihood of $\tilde{s}_{\mathrm{out_{NL}}}^{l}$ is obtained to solve for $\hat{s}_{\mathrm{out_{NL}}}^{l}$ as,

$$\begin{aligned} \hat{s}_{\mathrm{out_{NL}}}^{l} &= \arg\max_{\hat{s}_{\mathrm{out_{NL}}}^{l}} \prod_{t=1}^{T_{\mathrm{T2}_l}} f\left(\tilde{s}_{\mathrm{out_{NL}}}^{l}(t)\right) \\ &= \arg\min_{\hat{s}_{\mathrm{out_{NL}}}^{l}} \sum_{t=1}^{T_{\mathrm{T2}_l}} (\tilde{s}_{\mathrm{out_{NL}}}^{l}(t) - \hat{s}_{\mathrm{out_{NL}}}^{l})^2 \end{aligned} \tag{3.13}$$

where $f(.)$ is the probability density function (PDF), T_{T2_l} are the total number of received lth

symbol corresponding to symbol $s^{l}_{\text{out}_{\text{NL}}}$, $l = 1, 2$ in time T_{T2}.

With two unique kinds of symbol used in the pilot sequence, both impaired by the power amplifier distortions, their magnitudes are defined by the Rapp model in equation 3.3

$$|\hat{s}^{l}_{\text{out}_{\text{NL}}}| = \frac{|\hat{s}^{l}_{\text{out}}|}{\left[1 + \left(\frac{|\hat{s}^{l}_{\text{out}}|}{x_0}\right)^{2p}\right]^{\frac{1}{2p}}} \tag{3.14}$$

At this point, the parameters p and x_0 need to be estimated, which are specific to the particular transmitter. This method is followed for two purposes; one, is for the identification of the transmitter based on the estimated parameters and two, is to compensate the nonlinear distortions. For this purpose, equation 3.14 is solved with $l = 1, 2$. Considering equation 3.14 with $l = 1$ and rearranging, the estimate of x_0 (denoted as $\hat{x}_0$) would be

$$\hat{x}_0 = \frac{|\hat{s}^{1}_{\text{out}}|}{\left(\left(\frac{|\hat{s}^{1}_{\text{out}}|}{|\hat{s}^{1}_{\text{out}_{\text{NL}}}|}\right)^{2\hat{p}} - 1\right)^{\frac{1}{2\hat{p}}}} \tag{3.15}$$

Here, the equation requires the information of p to estimate x_0. To estimate $\hat{p}$, substitute $l = 2$ in equation 3.14 and $x_0 = \hat{x}_0$ from equation 3.15, and simplify to get

$$\begin{aligned}(|\hat{s}^{2}_{\text{out}}||\hat{s}^{1}_{\text{out}}||\hat{s}^{2}_{\text{out}_{\text{NL}}}|)^{2\hat{p}} - (|\hat{s}^{2}_{\text{out}}||\hat{s}^{1}_{\text{out}}||\hat{s}^{1}_{\text{out}_{\text{NL}}}|)^{2\hat{p}} + \\ (|\hat{s}^{1}_{\text{out}}||\hat{s}^{2}_{\text{out}_{\text{NL}}}||\hat{s}^{1}_{\text{out}_{\text{NL}}}|)^{2\hat{p}} - (|\hat{s}^{2}_{\text{out}}||\hat{s}^{2}_{\text{out}_{\text{NL}}}||\hat{s}^{1}_{\text{out}_{\text{NL}}}|)^{2\hat{p}} = 0\end{aligned} \tag{3.16}$$

Using the estimated parameters, $\hat{p}$ and $\hat{x}_0$, the power amplifier distortions are compensated by implementing it in the model described by equation 3.10. This is shown in the 'Nonlinear

Parameter Estimation' and 'Nonlinear Compensation' blocks of Fig. 3.4.

The parameter estimation model derived here require at least two unique symbols containing power amplifier distortions which can be obtained from any M-QAM. In the case of higher QAM, there are more than two unique outer symbols impaired by the power amplifier distortions, and thus all these symbols can be used in the pilot signal. For example, in a 64-QAM, there are 7 possible unique symbols with power amplifier distortion (Fig. 3.3). This results in $l > 2$ in equation 3.14 and can be solved for the power amplifier parameters p and x_0. Since, this would lead to an over-determined system, least squares methods like Levenberg−Marquardt algorithm can be used to solve for the power amplifier parameters.

Now, the estimated parameters $\hat{p}$ and $\hat{x}_0$, when communication was established with the intended transmitter, are considered as the device identification parameters of the transmitter and is used for its identification. Let it be called 'validated' power amplifier parameters denoted as $\psi_{val} \in \{\hat{p}_{val}, \hat{x}_{0_{val}}\}$.

3.4 Transmitter Identification Procedure

The transmitter is identified by its 'validated' radiometric power amplifier parameters defined by ψ_{val} as mentioned in Section 3.3. As long as the actual transmitter is communicating with the receiver, these values of ψ_{val} do not change. The basic idea for the device identification process is that the receiver re-estimates the power amplifier parameters periodically using the parameter estimation methodology proposed in this chapter and verifies with the validated power amplifier parameters. If the re-estimated parameters do not match with the validated one, it can be concluded that the current transmitter device is different from the validated transmitter. The identification of the transmitter is based on the two parameters of the power

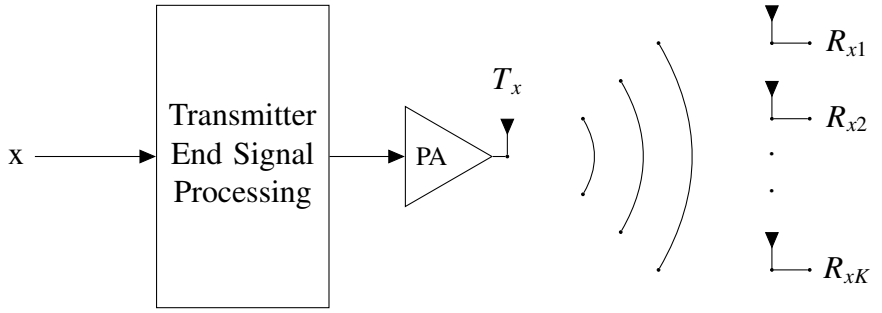

Figure 3.4: Identification Process by Collaboration of Receivers

amplifier, viz. $\{\hat{p}_{val}, \hat{x}_{0_{val}}\}$, and thus the identification process proposed in this paper is a robust method as both the re-estimated parameters have to match with the corresponding validated parameters. The identification is done with the collaboration of multiple receivers [12].

Considering K receivers as in Fig. 3.4, the receivers estimate the parameters and also compensate the distortions using the compensation mechanism given in this chapter. It is assumed that all K receivers have stored the same $\psi_{val} \in \{\hat{p}_{val}, \hat{x}_{0_{val}}\}$ of the transmitter [12]. During the identification process, the kth receiver re-estimates the power amplifier parameters $\psi_{est_k} \in \{\hat{p}_k, \hat{x}_{0,k}\}$. Ideally, ψ_{est_k} should match with ψ_{val} if the communication is still with the intended transmitter, but practically the estimated parameters may get corrupted by noise. Thus, the values ψ_{est_k} from K receivers follow a distribution. Based on the central limit theorem, it is considered that $\psi_{est_k} \sim \mathcal{N}(\bar{\psi}_{est}, \sigma^2_{\psi_{est}})$ for the analysis, with mean $\bar{\psi}_{est}$ and variance $\sigma^2_{\psi_{est}}$. For the case where the set of values follow a different distribution, analysis must be carried out for that case.

To identify the transmitter, a binary hypothesis test is modeled as

$$\begin{cases} \mathcal{H}_0 : \quad \bar{\psi}_{est} = \psi_{val} \\ \mathcal{H}_1 : \quad \bar{\psi}_{est} \neq \psi_{val} \end{cases} \tag{3.17}$$

Here $\mathcal{H}_0$ corresponds to the validated transmitter and $\mathcal{H}_1$ corresponds to a different transmitter parameters.

In order to solve this hypothesis model, the t-test is performed [46]. The criteria for the analysis using t-test is defined as

$$\begin{aligned} &\text{Reject } \mathcal{H}_0 \text{ if} \\ &|T_0| > t_{\alpha/2,K-1} \text{ or} \\ &|T_0| < -t_{\alpha/2,K-1} \end{aligned} \tag{3.18}$$

where T_0 and $t_{\alpha/2,K-1}$ are the test statistic and *t-value* (obtained from the t-distribution table) respectively evaluated from the set of estimated parameters, α is the 'significance level' defined as 'probability of rejecting $\mathcal{H}_0$ given that it is true', and $K-1$ are the degrees of freedom. α is typically chosen as 0.05, i.e. it is acceptable to have a 5% probability of incorrectly rejecting $\mathcal{H}_0$ [46]. T_0 follows a student t-distribution and is defined as [46]

$$T_0 = \frac{\bar{\psi}_{val} - \bar{\psi}_{est}}{\sqrt{\frac{\sigma^2_{\psi_{est}}}{K}}} \tag{3.19}$$

In the event of change in transmitter, $\mathcal{H}_1$ gets acquired upon the application of this test and when this happens, the receivers take a decision that the current transmitter is different from the validated transmitter. By the t-test, the confidence interval (CI) for the parameters of the validated transmitter is given by

$$\text{CI} = \bar{\psi}_{est} \pm t_{\alpha/2,K-1} \sqrt{\frac{\sigma^2_{\psi_{est}}}{K}} \tag{3.20}$$

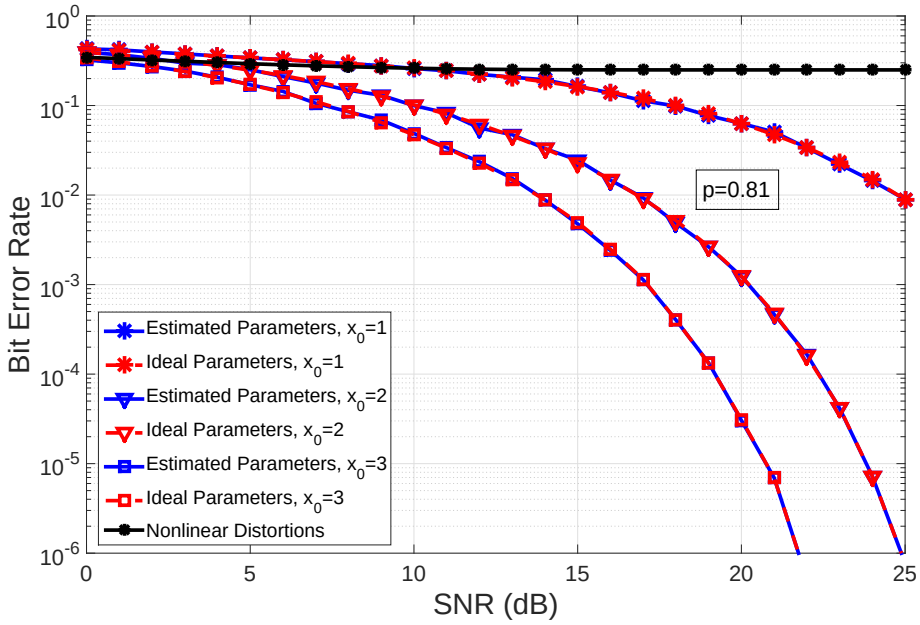

Figure 3.5: Performance of 16-QAM STBC System with Proposed Compensation Technique, $n_{tr} = n_r = 2$, p=0.81

The error probability is given by

$$\beta = P\{-t_{\alpha/2,K-1} \leq T_0 \leq t_{\alpha/2,K-1} \text{ when } \delta \neq 0\} \tag{3.21}$$

where δ is the non-centrality parameter. The power of the statistical test is given by $1 - \beta$.

3.5 System Implementation and Simulation Results

3.5.1 Compensator Performance

The system was simulated in MATLAB® with a 16-QAM and 64-QAM MIMO-STBC system with $n_{tr} = 2$ and $n_r = 2$ and a MIMO channel. One million data symbols were considered

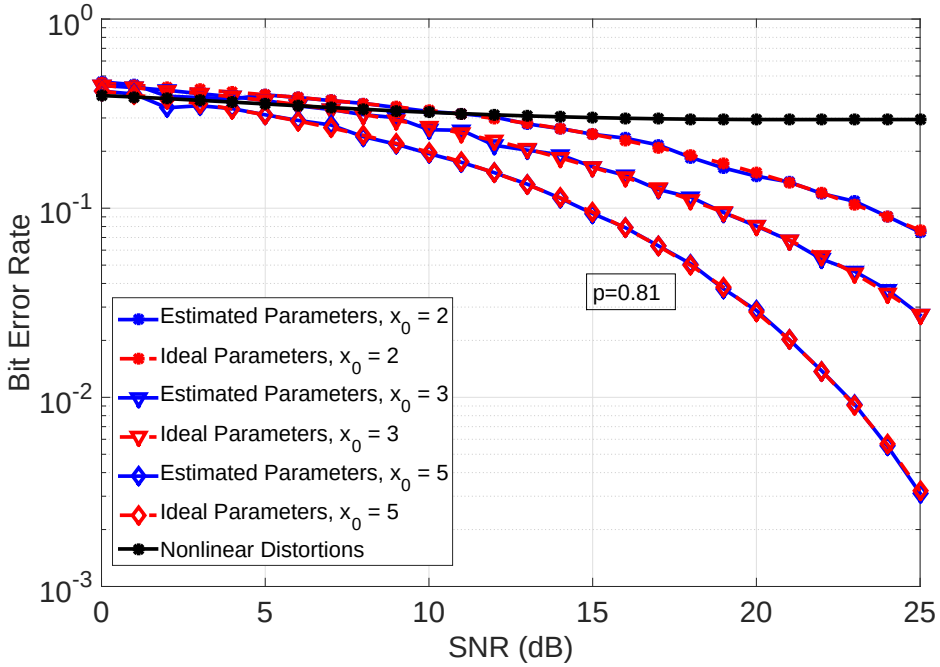

Figure 3.6: Performance of 64-QAM STBC System with Proposed Compensation Technique, $n_{tr} = n_r = 2$, p=0.81

of which thirty thousand symbols were used as pilot symbols with s_1, s_2 and s_3 each as ten thousand. The power amplifier parameters namely the smoothness factor was $p = 0.81$ [47], and was simulated at different levels of x_0 namely $x_0 = 1, 2$ and 3 for a 16-QAM and $x_0 = 2, 3$ and 5 for the 64-QAM to evaluate the performance of the compensation mechanism. $x_0 = 1$ was not considered for a 64-QAM as this value would drive the power amplifier to deep saturation which is not the usual operation range of power amplifiers. The pilot signal X^{T1} was assumed to make a perfect channel estimate for every symbol duration T. X^{T1} needs to be transmitted with every time frame to track the fast changes in the channel while X^{T2} can be transmitted only once to estimate the power amplifier model parameters because once the parameters are estimated, it is unique to the transmitter and needs to be estimated again only to verify if the transmitter is still the validated one or a different one. This would significantly improve the

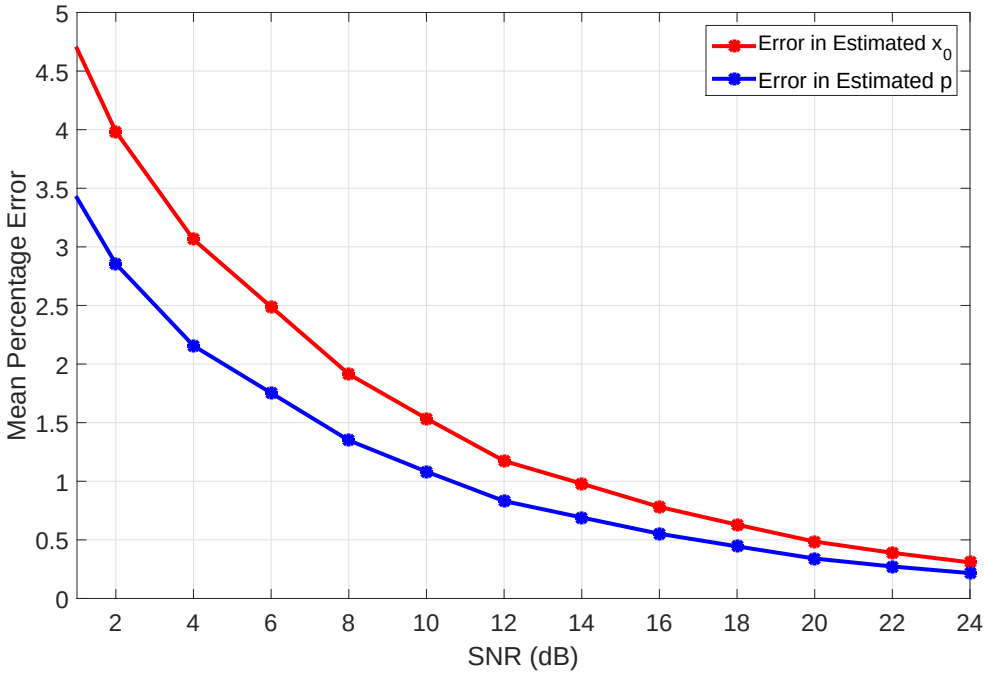

Figure 3.7: Error in Estimated PA Parameters as a Function of SNR

bandwidth efficiency of the system and reduce the signal processing complexity at the receiver. The nonlinear distortion parameters were estimated using the proposed algorithm and were applied to the inverse model defined in equation 3.10 to compensate the distortions. Fig. 3.5 and Fig. 3.6 shows the performance of the 16-QAM and 64-QAM MIMO STBC system in terms of Bit Error Rate (BER) with respect to Signal-to-Noise Ratio (SNR) at various levels of x_0. The plot gives the comparison of the performance with and without distortion compensation. It is seen that the proposed system has better performance for a higher x_0 due to a higher back-off. The dotted curve indicate the performance with ideal (known) parameters of the power amplifier and the solid line indicates the performance with estimated parameters of the power amplifier. In both the plots, the plots match and show a good performance in terms of distortion compensation. Fig. 3.7 shows the plot of error percentage between the estimated and ideal

values of the power amplifier parameters p and x_0 as a function of signal-to-noise ratio when the estimation is done using the pilot signal X^{T2} using 1000 trials. Good performance here is defined as a bit error rate value of less than 5% for typical working ranges of signal-to-noise ratio (>18dB)

3.5.2 Transmitter Identification Process Performance

The simulation setup for testing the device identification process consisted of the validated parameters $p = 0.81$ and $x_0 = 2$ with a 16-QAM system and the parameters for the different transmitter as $p = 0.9$ and $x_0 = 3$ with the collaboration of 8 receivers. The t-test successfully identified the transmitter with $p = 0.9$ and $x_0 = 3$ as a transmitter different from the validated one. To test the performance of the proposed identification process at different noise levels, the power of the statistical t-test (probability of rejecting the transmitter) as a function of the differences between the validated and estimated parameters was plotted, at different standard deviation of $\sigma_{\psi_{est}} = 0.25, 0.5, 1$ and 2 and is shown in Fig. 3.8 (The standard deviation is obtained as the square root of the variance of ψ_{est_k}). It is seen that the power of t-test is high when the difference in parameters is high and increases sharply for low variance (low noise levels). This means that at low noise levels, even the slightest variation in power amplifier parameters outside the CI is easily identified. Typically the variance of the sample distribution from the estimated values were found to be in a very low range of 0.017 (as seen from simulations) because the parameters are estimated after compensation of channel AWGN in (3.13) using the maximum likelihood method and thus the effect of channel noise is very minimal. The noise may creep in only due to rounding-off errors during the mathematical processing.

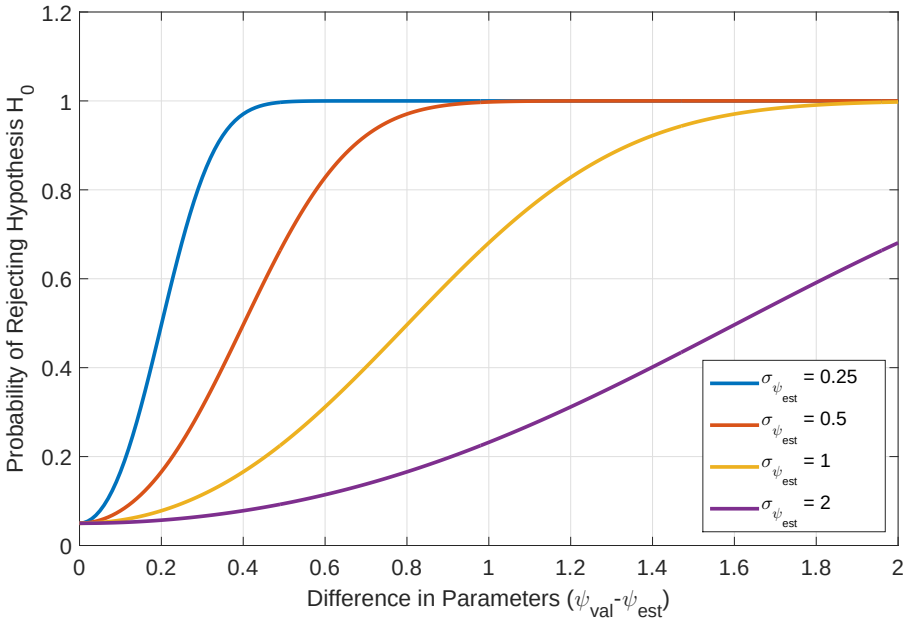

Figure 3.8: Performance of t-test in terms of Identifying the Non-Validated Transmitter

3.6 Effectiveness of Nonlinear Compensator for Variations in Parameter Values

This section speaks about the effectiveness of the proposed compensation method when the power amplifier operate at different values of parameters, viz., saturation level parameter x_0 and smoothness factor p. The variation of these values occur based on the type of power amplifier and its biasing conditions at the transmitter. In order to analyze the effectiveness of the performance of the system for variation of these parameters, the system was simulated for a range of values of a parameter keeping the other parameters constant. Thus, the sensitivity of p was studied by keeping x_0 constant and varying p through a range. The same was done for x_0 by keeping p constant. Fig. 3.5 and Fig. 3.9 shows the performance of the system for variation of parameter values of p and x_0 respectively for a 16-QAM system.

3.6.1 Effect of p

Parameter p defines how smoothly the characteristics of the power amplifier change from the linear region to the nonlinear region. The value of p is primarily dependent on the type of transistor used in the power amplifier. Lower value of p denotes a smoother transition whereas a larger value depicts a sharp transition as illustrated in Fig. 2.8. From IEEE standards documentation, the typical values of p lie between 2 and 3 for a practical power amplifier depending on the type of the transistor used [48] but a particular standard is defined for power amplifiers used in 802.11 applications which is defined as $p = 0.81$ [47]. A test case of $p = 1.02$ has also been considered for simulations in literature [49]. A good performance of the proposed compensation mechanism at these ranges of p would make this compensation mechanism a practical solution.

To analyze the effect of variation of p on the system performance using the proposed compensation mechanism, simulations were done using this system by setting the practical extreme possible values of p (p values as 0.81, 1.02, 2, 3) and the performance in terms of Bit Error Rate (BER) was plotted to evaluate the effectiveness of the proposed model practically. The value of x_0 was set as 2.5. It was observed that the drop in BER as a function of Signal to Noise ratio (SNR) is late for a power amplifier working at high smoothness factor. This means a signal distorted by power amplifier distortions due to a high value of p need a high SNR signal to compensate the distortions effectively. From equation 3.9 it can be noted that the power amplifier working at a very high smoothness factor p (In this case $p = 3$) requires a signal with high SNR (In this case 35dB) for an acceptable level of performance while power amplifiers working at very low smoothness factors start giving a significantly good performance at low SNR levels which is a good point to be noted. When it comes to practical power amplifiers with

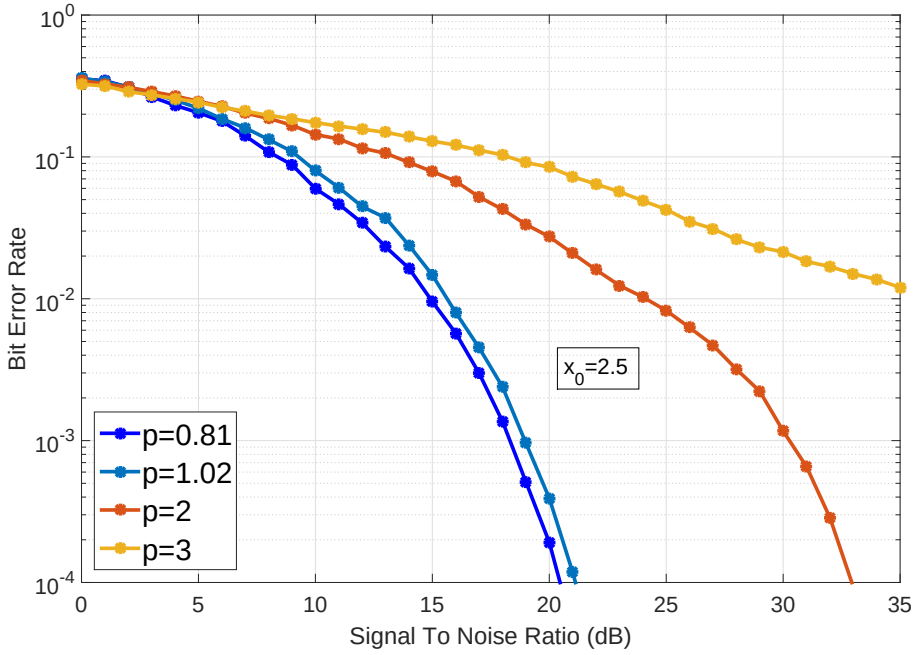

Figure 3.9: Performance of the system at various p at x_0=2.5

p between 2 and 3, an acceptable level of performance is still achieved in 16-QAM systems as shown in Fig. 3.9. The yellow curve is the performance of the power amplifier working at the upper bound of the practical range of power amplifiers ($p = 3$).

Thus, it can be concluded that the effectiveness of the proposed compensation mechanism is dependent on p; its performance reduces with increase in the value of the smoothness factor p. Based on the tests for the standard practical working ranges of p, the proposed compensation mechanism can be effectively implemented in practical receivers.

3.6.2 Effect of x_0

Parameter x_0 is the factor which defines the saturation level at which the power amplifier is working. This value is dependent on the operating conditions such as the biasing voltage and

saturation level at which the power amplifier is operated at the transmitter. The lower value of x_0 is equivalent to a deeper saturation level which leads to higher clipping of signals and higher loss of data in the signal; in other words, the power amplifier is working at very low back-offs. Thus, a very low value of x_0 leads to significant degradation of the signal, that the compensation mechanism will not be effective enough to compensate these distortions, leading to poorer performance of the system. The value of x_0 is adjustable by the user at the transmitter and is generally set at an optimized range of values as explained in Section 2.3.

The system performance due to the effect of variation of x_0 can be seen from Fig. 3.5 which is simulated at three values of the saturation level parameter $x_0 = 1, 2, 3$ and maintaining $p = 0.81$. It may be noted from Fig. 3.5 that the drop in the BER curve as a function of SNR is steeper for a signal working at a higher x_0 ($x_0 = 3$), because less data in the signal is lost due to clipping. Lower values of x_0 drives them to deeper saturation and the drop in the BER curve is less steep.

From Fig. 3.5 and Fig. 3.6, it can be concluded that as the saturation level of the power amplifier reduces, the power amplifier works at very low back-off and the effectiveness of the proposed technique reduces. Practically, power amplifiers are made to work at an optimized saturation levels as explained in Section 2.3. Given that the power amplifier is operated at near saturation levels, the proposed compensation mechanism is effectively implemented at close to these values of saturation levels and the parameters are effectively estimated.

3.7 Summary

This chapter proposes a methodology of identification of the source of distortion in a wireless communication system and its compensation considering the power amplifier and the channel

distortions using a two-step pilot signal approach. The motive behind this methodology is to identify the 'fairly static' and dynamic distortions separately, and develop a distortion compensation model with lower complexity. A lower complexity is achieved since the power amplifier parameters are identified once and are re-used for all other symbols for compensation instead of re-estimating them again and again. The simulations verify that the proposed method has a robust performance in terms of bit error rate. This section also illustrates the effect of the power amplifier parameters, when power amplifiers work at that levels.

This technique was also developed and implemented for a transmitter identification procedure, based on the information of the estimated parameters of the power amplifier. A statistical t-test was used to compare the parameters to identify the transmitter. Computer simulations show its implementation and successful identification of the transmitter device. The proposed method can be implemented in conjunction with other physical layer device identification methods for intended transmitter identification with an enhanced performance.

Chapter 4

Millimeter-wave OFDM system with Power Amplifier Nonlinearity

4.1 Introduction

Power amplifiers are an integral part of communication systems to increase the strength of signals transmitted into the wireless media. These power amplifiers produce nonlinear distortions due to their saturation nature and are widely produced in OFDM systems due to their high Peak to Average Power Ratio (PAPR) operation. The behavior of power amplifiers also varies with the frequencies at which they operate. Most of the present communication systems work in Ultra High Frequency (UHF) range and are defined by power amplifier behavioral models such as the Rapp model, Saleh model etc. as discussed in Chapter 2. Extensive work on the theoretical analysis of power amplifier performance has been carried out by Bohara for the UHF range [9] [50] [51]. This work needs to be extended to the millimeter wave communication systems due to upcoming technologies in this area.

With the demand for higher data rates and limited spectrum available, technologies are being developed in the millimeter wave range of signals to achieve higher bandwidths. In this chapter, the performance of millimeter wave Orthogonal Frequency Division Multiplexing

(OFDM) wireless communication systems in presence of power amplifier nonlinear distortions is studied. Practical analysis of a millimeter wave power amplifiers is more complex than UHF systems at this point of time due to hardware availability issues and complex simulation processes, and thus need mathematical models for their analyses. The modified Bessel-Fourier series model, which models the behavior of millimeter wave power amplifiers considering the equivalent stray effects of high frequency operation, has been used here to derive an analytical expression for the symbol error probability which evaluates the performance of millimeter wave communication systems in presence of power amplifier distortions. This expression can be used to avoid the cumbersome evaluation of the system performance from complex simulations [34]. The results of the analytical expression is compared to the simulation values of the communication system and verified. This is followed by a methodology to obtain the equivalent parameters for the Rapp model for a millimeter wave system.

The chapter is organized as follows. Section 4.2 describes the system model considered for the implementation, Section 4.3 gives the derivation details of the theoretical analysis of the system followed by its simulation and verification in Section 4.4. Section 4.5 derives the equivalent parameters for the Rapp model for the millimeter wave power amplifier modeled using the modified Bessel-Fourier series. The summary of the chapter is given in Section 4.6.

4.2 System Model

A millimeter wave OFDM system impaired by the power amplifier is considered as shown in Fig. 4.1. The millimeter wave communication signal is subject to power amplifier nonlinearity and a wireless channel.

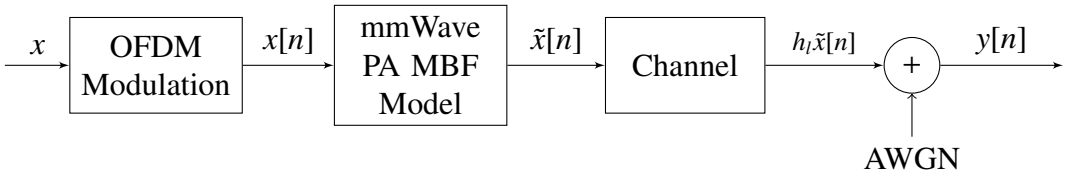

Figure 4.1: System Model of mmWave Transceiver with Power Amplifier Impairments

An OFDM signal is given by [9]

$$x[n] = \begin{cases} \frac{1}{N}\sum_{m=0}^{N-1} X_m e^{\frac{j2\pi mn}{N}} & \text{for} - N_g \leq n \leq N-1 \\ 0 & \text{otherwise} \end{cases} \tag{4.1}$$

where n is time index, N is the Inverse Fast Fourier Transform (IFFT) length of the OFDM system, N_g is the guard interval length, X_m is the complex data symbol in frequency domain in the mth subcarrier.

Expressing this OFDM signal in terms of its magnitude and phase at a given time index n, by converting it to the polar form, $x[n]$ in equation 4.1 can be written as

$$x[n] = |x[n]|e^{j\theta} \tag{4.2}$$

where $|x[n]|$ is the magnitude of the signal and θ is the phase of the signal. It is assumed that X_m are independent and identically distributed with zero mean and variance σ^2 [50]. Thus, when N is large, $x[n]$ can be assumed to be a complex Gaussian process with zero mean and variance $P_{av} = \sigma^2/N$ [9]. The polar form is considered because the effect of the power amplifier is on the magnitude of the signal.

4.3 Analytical Performance of the System

In this section, the details of the analysis of the system in Fig. 4.1 is discussed and the analytical expression for performance evaluation of this system in terms of symbol error probability has been derived. First, the model considered for the millimeter wave power amplifier is discussed followed by its implementation to analytically arrive at the expression.

4.3.1 Power Amplifier Distortions

The power amplifier model implemented for this OFDM system uses the modified Bessel-Fourier (MBF) series model described in [37]. It has been established that the MBF series model is the most suited model for modeling millimeter wave power amplifiers with the help of actual Laterally Diffused Metal Oxide Semiconductor (LDMOS) power amplifier measurements [34]. Hence, the MBF model can been considered for the analysis.

The OFDM signal $x[n]$ in the time domain is passed through the power amplifier before transmission to the wireless channel. Considering a millimeter wave signal, the output of the power amplifier with nonlinear distortions, modeled by the MBF series model is given by [34][37]

$$\tilde{x}[n] = \sum_{p=1}^{P} b_{(2p-1)} J_1\left(\frac{2\pi}{\gamma D}(2p-1)|x[n]|\right) e^{j\theta} \tag{4.3}$$

where $\tilde{x}[n]$ is the nonlinearly distorted signal appearing at the output of the power amplifier, P is the Bessel-Fourier series order, $b_{(2p-1)}$ is the $(2p-1)$ th coefficient of the Fourier series approximation, $J_1(.)$ is the Bessel function, γ is the dynamic range ratio parameter and D is the dynamic range of the power amplifier. $|x[n]|$ and θ are the magnitude and phase of the signal respectively.

The optimum Bessel-Fourier series order for modeling a LDMOS power amplifier is the third order model ($P = 3$) [37]. Thus, nonlinearly distorted output OFDM signal after substituting for P in equation 4.3 gives

$$\tilde{x}[n] = \Big(b_1 J_1(\alpha|x[n]|) + b_3 J_1(3\alpha|x[n]|) + b_5 J_1(5\alpha|x[n]|)\Big)e^{j\theta} \tag{4.4}$$

where $\alpha = 2\pi/\gamma D$ [37].

With the intention to analyze the current system and to derive the analytical expression for the symbol error probability, the MBF series model is expressed in the form of a polynomial model by expanding the Bessel functions with its Taylor series [52]. Expanding and simplifying equation 4.4 results in

$$\begin{aligned}\tilde{x}[n] = |x[n]|\frac{\alpha}{2}\Bigg\{ & b_1\left(1 - \frac{(\alpha|x[n]|)^2}{8} + \frac{(\alpha|x[n]|)^4}{192} + ...\right) \\ & + 3b_3\left(1 - \frac{(3\alpha|x[n]|)^2}{8} + \frac{(3\alpha|x[n]|)^4}{192} + ...\right) \\ & + 5b_5\left(1 - \frac{(5\alpha|x[n]|)^2}{8} + \frac{(5\alpha|x[n]|)^4}{192} + ...\right)\Bigg\}e^{j\theta}\end{aligned} \tag{4.5}$$

Here, since $|x[n]|e^{j\theta}$ is the polar form of the signal $x[n]$, from (4.2), it can written as $x[n]$. Thus, with this substitution and rearrangement, equation 4.5 becomes

$$\begin{aligned}\tilde{x}[n] &= x[n]\frac{\alpha}{2}\Bigg\{(b_1 + 3b_3 + 5b_5) - \frac{(\alpha|x[n]|)^2}{8}(b_1 + 27b_3 + 125b_5) + \\ &\quad \frac{(\alpha|x[n]|)^4}{192}(b_1 + 243b_3 + 3125b_5) - ...\Bigg\} \\ &= x[n]\frac{\alpha}{2}\Big\{c_1 - c_2(|x[n]|)^2 + c_3(|x[n]|)^4 - ...\Big\}\end{aligned} \tag{4.6}$$

where $c_1 = b_1 + 3b_3 + 5b_5$, $c_2 = (\alpha^2/8) * (b_1 + 27b_3 + 125b_5)$ and $c_3 = (\alpha^4/192) * (b_1 + 243b_3 + 3125b_5)$. Here α, c_1, c_2, c_3 are model parameters which are power amplifier dependent.

The Taylor series form of the function in equation 4.6 is considered up to the third order of nonlinearity. This is because power amplifiers in OFDM systems are operated at near saturation levels and not in deep saturation which are studied using third order polynomial models. Thus, the output of the millimeter wave power amplifier impaired by nonlinear distortions can be considered up to the third order nonlinearity, and approximated as

$$\tilde{x}[n] \approxeq \left(\frac{\alpha c_1}{2}\right) x[n] + \left(\frac{-\alpha c_2}{2}\right) x[n]|x[n]|^2 + \dots \tag{4.7}$$

where $\alpha c_1/2$, $-\alpha c_2/2$ are the co-efficients of the order of nonlinearities. This is of the form of the polynomial model given by [25]

$$\tilde{x}[n] = \sum_{d=1}^{D} a_{2d-1} x[n]|x[n]|^{2(d-1)} \tag{4.8}$$

where $d = 1, 2, 3, ...$ is the order of nonlinearity.

The co-efficients $a_1, a_3 \dots$ for this polynomial model are defined as $\alpha c_1/2, \alpha c_2/2 \dots$ respectively, applicable to millimeter wave signals.

4.3.2 Channel Distortions

The signal containing the nonlinear distortions passes through the multi-path wireless channel before reaching the receiver. The multi-path is modeled as a finite impulse response filter with L taps, where each tap denote each of the multi-path traversed by the signal [2].

The millimeter wave OFDM signal containing nonlinear distortions, $\tilde{x}[n]$, passes through the multi-path channel and the received signal can be written as

$$y[n] = \sum_{l=1}^{L} h_l \tilde{x}[n - \tau_l] + w_l \tag{4.9}$$

where l are the number of paths, h_l is the channel response of the lth path, τ_l is the time delay on $l-$th path, $\tilde{x}[n]$ is the signal with nonlinear distortions and w_l is the Additive White Gaussian Noise (AWGN) in the $l-$th path.

Taking Discrete Fourier Transform (DFT), and simplifying, the received signal in the mth subcarrier is written as

$$\begin{aligned} Y_m &= \sum_{n=0}^{N-1} \sum_{l=1}^{L} h_l \tilde{x}[n - \tau_l] e^{-\frac{j2\pi mn}{N}} + w_l[m] \\ &= \sum_{n=0}^{N-1} \sum_{l=1}^{L} h_l \left(\frac{\alpha c_1}{2}\right) x[n - \tau_l] e^{-\frac{j2\pi mn}{N}} \\ &+ \sum_{n=0}^{N-1} \sum_{l=1}^{L} h_l \left(\frac{-\alpha c_2}{2}\right) x[n - \tau_l] |x[n - \tau_l]|^2 e^{-\frac{j2\pi mn}{N}} + w_l[m] \end{aligned} \tag{4.10}$$

$w_l[m]$ corresponds to DFT equivalent of AWGN in the mth subcarrier.

Using circular time shift property of Discrete Fourier Transform (DFT), the received signal is given by

$$\begin{aligned} Y_m &= \sum_{l=1}^{L} h_l \left(\frac{\alpha c_1}{2}\right) \sum_{n=0}^{N-1} x[n] e^{-\frac{j2\pi mn}{N}} e^{-\frac{j2\pi m\tau_l}{N}} \\ &+ \sum_{l=1}^{L} h_l \left(\frac{-\alpha c_2}{2}\right) \sum_{n=0}^{N-1} x[n] |x[n]|^2 e^{-\frac{j2\pi mn}{N}} e^{-\frac{j2\pi m\tau_l}{N}} + w_l[m] \end{aligned} \tag{4.11}$$

Considering $|x[n]|^2 = \gamma_n$ and with some simplification [9] (Refer Appendix.A),

$$\begin{aligned} Y_m =& X_m \sum_{l=1}^{L} h_l \left[\left(\frac{\alpha c_1}{2} \right) - \left(\frac{\alpha c_2}{2N} \right) \sum_{n=0}^{N-1} \gamma_n \right] e^{-\frac{j2\pi m\tau_l}{N}} \\ &+ \sum_{l=1}^{L} h_l \left(\frac{-\alpha c_2}{2N} \right) \sum_{\substack{q_1=0 \\ q_1 \neq m}}^{N-1} X_{q_1} \sum_{n=0}^{N-1} \gamma_n e^{\left(\frac{j2\pi(q_1-m)n}{N}\right)} e^{-\frac{j2\pi m\tau_l}{N}} + w_l[m] \end{aligned} \tag{4.12}$$

Denoting equation 4.12 as below, the received signal is represented as

$$Y_m = X_m \sum_{l=1}^{L} \mu_l + \sum_{l=1}^{L} \eta_l + w_l[m] \tag{4.13}$$

where the terms μ_l and η_l are given by equation 4.14 and equation 4.15 respectively each denoting the linear attenuation component and the nonlinear distortion component respectively.

$$\mu_l = h_l \left[\left(\frac{\alpha c_1}{2} \right) - \left(\frac{\alpha c_2}{2N} \right) \sum_{n=0}^{N-1} \gamma_n \right] e^{-\frac{j2\pi m\tau_l}{N}} \tag{4.14}$$

$$\eta_l = h_l \left[\left(\frac{-\alpha c_2}{2N} \right) \sum_{n=0}^{N-1} \gamma_n \sum_{\substack{q_1=0 \\ q_1 \neq m}}^{N-1} X_{q_1} e^{\frac{j2\pi(q_1-m)n}{N}} \right] e^{-\frac{j2\pi m\tau_l}{N}} \tag{4.15}$$

This expression separates the linear attenuation, nonlinear distortion and the Additive White Gaussian Noise components of the received signal. The linear component is the desired component of the signal and the undesired components include the nonlinear distortion component and noise of the signal. These information are used for further analysis of the system.

4.3.3 Symbol Error Probability Analysis

Various quantities of the system output are considered for performance analysis of communication systems. In this analytical expression derivation, the performance of the system in terms of symbol error probability has been considered. The relation for the symbol error probability P_{Se} of an M-QAM system per carrier is given by [53]

$$P_{Se} = 2\left(1 - \frac{1}{\sqrt{M}}\right) Q\left(\sqrt{\frac{3SNR}{(M-1)}}\right) \tag{4.16}$$

where $Q(.)$ is the Gaussian Q-function, SNR is the signal-to-noise ratio, M is the number of constellation points in a QAM.

Evaluation of the symbol error probability in equation 4.16 requires the value of signal-to-noise ratio which is calculated theoretically from the information of the linear desired signal component and nonlinear distortion components of the received signal in equation 4.12. The linear signal and the nonlinear distortion components are modeled as zero mean Gaussian process [9]. Hence, the variance of the signal is the expected value of the squared signal. Thus, the signal to noise ratio for each subcarrier of the system is calculated as [9]

$$SNR = \frac{\sigma^2 E\left[\left|\sum_{l=1}^{L} \mu_l\right|^2\right]}{\sigma_{NL}^2 + W_m} \tag{4.17}$$

where σ_{NL}^2 is the variance of the nonlinear component of the signal and W_m is AWGN.

Since nonlinear distortions are independent of the channel distortions, the expected value

of the desired component squared is calculated as,

$$\begin{aligned} E\left[\left|\sum_{l=1}^{L}\mu_l\right|^2\right] &= E\left[\left|\sum_{l=1}^{L}h_l e^{-\frac{j2\pi m\tau_l}{N}}\right|^2\right]E\left[\left|\left(\frac{\alpha c_1}{2}\right)-\left(\frac{\alpha c_2}{2N}\right)\sum_{n=0}^{N-1}\gamma_n\right|^2\right] \\ &= \psi[m]\left\{E\left[\left|\left(\frac{\alpha c_1}{2}\right)\right|^2\right]+\left(\frac{\alpha c_2}{2N}\right)^2 E\left[\left|\sum_{n=0}^{N-1}\gamma_n\right|^2\right]-\left(\frac{c_1c_2\alpha^2}{2N}\right)E\left[\left|\sum_{n=0}^{N-1}\gamma_n\right|\right]\right\} \end{aligned} \tag{4.18}$$

where $\psi[m] = E\left[\left|\sum_{l=1}^{L}h_l e^{-\frac{j2\pi lm}{N}}\right|^2\right]$, σ^2 is the variance of X_m.

Here $\alpha c_1/2$ and $-\alpha c_2/2N$ are constants specific to the power amplifier and hence, their expected values are the value itself. The expected value of $\sum_{n=0}^{N-1}\gamma_n = \sigma^2$ and $\sum_{n=0}^{N-1}\gamma_n^2 \cong (\sigma^2)^2$. (Ref. Appendix A). Thus, the numerator of equation 4.17 becomes,

$$\sigma^2 E\left[\left|\sum_{l=1}^{L}\mu_l\right|^2\right] = \sigma^2\psi[m]\left[\left(\frac{\alpha c_1}{2}\right)^2+\left(\frac{\alpha c_2}{2N}\right)^2(\sigma^2)^2-\left(\frac{c_1c_2\alpha^2}{2N}\right)\sigma^2\right] \tag{4.19}$$

The denominator in equation 4.17 is noise, which is the sum of the expected value of nonlinear component and AWGN. The expected value of the nonlinear component is derived as [9]

$$\begin{aligned} E\left[|\eta_l|^2\right] &= E\left[\left|\frac{1}{N}\sum_{l=1}^{L}h_l\left(\frac{-\alpha c_2}{2}\right)e^{-\frac{j2\pi lm}{N}}\sum_{n=0}^{N-1}\gamma_n\sum_{\substack{q_1=0\\q_1\neq m}}^{N-1}X_{q_1}e^{\frac{j2\pi(q_1-m)n}{N}}\right|^2\right] \\ &= E\left[\left|\left(\frac{-\alpha c_2}{2N}\right)\right|^2\right]E\left[\left|\sum_{l=1}^{L}h_l e^{-\frac{j2\pi lm}{N}}\right|^2\right]E\left[\left|\sum_{n=0}^{N-1}\gamma_n\sum_{\substack{q_1=0\\q_1\neq m}}^{N-1}X_{q_1}e^{(\frac{j2\pi(q_1-m)n}{N})}\right|^2\right] \end{aligned} \tag{4.20}$$

since X_{q_1} is independent of the channel distortions and the coefficient $-\alpha c_2/2N$ of the terms.

Again, in this expression, the expected value of the constant $-\alpha c_2/2N$ is itself, the expected value of the channel is obtained from the channel estimation. The expected value of the third term is calculated as follows. The derivation details are given in [9]

$$\begin{aligned} & E\left[\left|\sum_{n=0}^{N-1}\gamma_n \sum_{\substack{q_1=0 \\ q_1\neq m}}^{N-1} X_{q_1} e^{\frac{j2\pi(q_1-m)n}{N}}\right|^2\right] \\ & = E\left[\sum_{\substack{q_1=0 \\ q_1\neq m}}^{N-1}\sum_{n=0}^{N-1}\gamma_n X_{q_1} e^{(\frac{j2\pi(q_1-m)n}{N})} \sum_{\substack{q_1=0 \\ q_1\neq m}}^{N-1}\sum_{n=0}^{N-1}\gamma_n X_{q_1}^* e^{(\frac{j2\pi(q_1-m)n}{N})}\right] \end{aligned} \tag{4.21}$$

Writing this as,

$$E\left[\sum_{\substack{q_1=0 \\ q_1\neq m}}^{N-1} R_{q_1} \sum_{\substack{q_1=0 \\ q_1\neq m}}^{N-1} R_{q_1}^*\right] \tag{4.22}$$

where

$$R_{q_1} = \sum_{n=0}^{N-1}\gamma_n X_{q_1} e^{\left(\frac{j2\pi(q_1-m)n}{N}\right)}$$

Thus, (4.21) becomes [9],

$$E\left[\sum_{\substack{q_1=0 \\ q_1\neq m}}^{N-1} R_{q_1} \sum_{\substack{q_1=0 \\ q_1\neq m}}^{N-1} R_{q_1}^*\right] = (N-1)\sigma_{q_1q_1}^2 + (N-1)(N-2)C_{q_1q_2} \tag{4.23}$$

where $\sigma_{q_1q_1}^2$ is the variance and $C_{q_1q_2}$ is the covariance.

The variance and covariance is given by [9].

$$\sigma^2_{q_1 q_1} = \gamma[m]\frac{(N+2)(\sigma^2)^3}{N^4} \tag{4.24}$$

$$C_{q_1 q_2} = \gamma[m]\frac{2(\sigma^2)^3}{N^4} \tag{4.25}$$

Substituting (4.24) and (4.25) in (4.23) and simplifying [9]

$$E\left[\left|\sum_{n=0}^{N-1}|x[n]|^2\sum_{\substack{q_1=0\\q_1\neq m}}^{N-1}X_{q_1}e^{(\frac{j2\pi(q_1-m)n}{N})}\right|^2\right] = \frac{\left(\sigma^2\right)^3\left(3N^2-5N+2\right)}{N^4} \tag{4.26}$$

Inserting equation 4.26 in equation 4.20, simplifying and substituting the simplified form along with equation 4.19 in equation 4.17, the signal-to-noise ratio of the system is given by

$$SNR = \frac{\psi[m]\sigma^2\left[\left(\frac{\alpha c_1}{2}\right)^2+\left(\frac{\alpha c_2\sigma^2}{2N}\right)^2-\left(\frac{c_1c_2\alpha^2\sigma^2}{2N}\right)\right]}{\left(\psi[m]\frac{\alpha^2c_2^2(\sigma^2)^3(3N^2-5N+2)}{4N^4}\right)+W_m} \tag{4.27}$$

which is used in equation 4.16 to evaluate the symbol error probability. Thus, using equation 4.27, the performance of the system can be evaluated with only the knowledge of the IFFT length, channel state information, variance of data symbols and the parameters of the power amplifier used, avoiding complex simulations.

For a channel with only AWGN, the term $\psi[m] = 1$ [9]. But in a multi-path channel, the symbol error probability is dependent on the channel state information $\psi[m]$. Knowing the probability distribution of the channel, the performance in presence of the channel distortions can be obtained. As an example, assuming a Rayleigh channel, the probability of symbol error

of the system can be written as [9],

$$\begin{aligned} f_s(m, \psi[m]) &= \int_0^\infty f_s p(\psi) \\ &= \int_0^\infty f_s \frac{1}{\theta} e^{-\psi/\theta} d\psi \end{aligned} \tag{4.28}$$

where $p(\psi)$ is the probability density of the channel, θ and ψ are the parameters of the probability density function of the Rayleigh distribution.

4.4 Simulations

The system was simulated in MATLAB® to verify the equation 4.27 obtained for the symbol error probability with the simulation values. A 16-QAM modulated Orthogonal Frequency Division Multiplexing (OFDM) system of Inverse Fast Fourier Transform (IFFT) lengths $N = 64$ and 128 having a perfect channel estimate was considered ($\psi[m] = 1$ for a perfect channel estimate [9]), each simulated at two levels of input back-off (IBO). The parameter α was set as 0.6, the optimum parameter for modeling power amplifiers using Bessel-Fourier series models as this value of α reasonably covers the dynamic range of the power amplifier [40]. The parameters c_1 and c_2 are calculated from equation 4.6. The results are shown in Fig. 4.2 and Fig. 4.3. The dotted curves represent the practical values from computer simulations and the solid curve is obtained from the analytical expression in equation 4.27. It is found that the practical values and the values obtained from the derived expression in this paper match very closely with the highest absolute error being about $2.5e10^{-4}$. The small variations in the values is due to the Bessel function approximation.

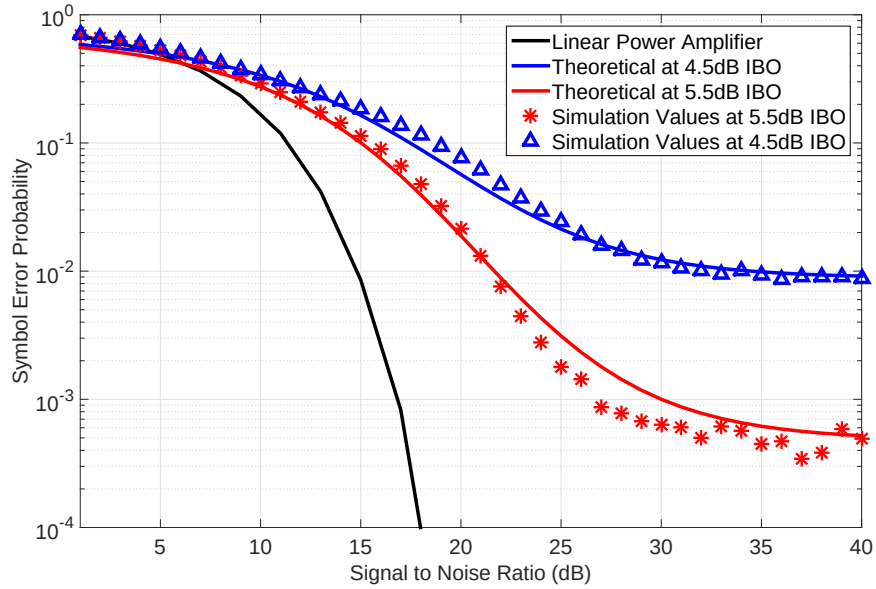

Figure 4.2: Plot of P_{Se} vs. SNR for different IBO with N=64

The input back-off is given by [9]

$$IBO = \frac{A^2}{P_{av}} \tag{4.29}$$

where A is the input amplitude for which the output power is maximum, P_{av} is the average power of the signal. The average power P_{av} is given by [9]

$$P_{av} = \frac{\sigma^2}{N} \tag{4.30}$$

where N is the IFFT length and σ^2 is the variance of the complex data symbols of each subcarrier.

The IBO of the system is dependent on the input amplitude A and hence can be varied by varying A. The IBO is also indirectly dependent on the IFFT length N. Thus, two cases of IFFT

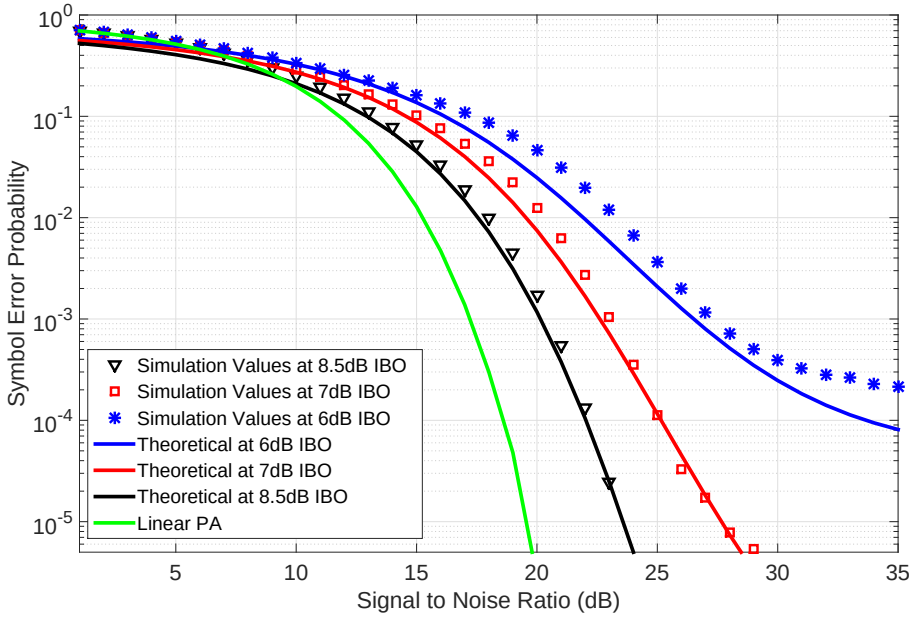

Figure 4.3: Plot of P_{Se} vs. SNR for different IBO with N=128

length N were considered for simulations and in each case, the power amplifier was operated at a different level of IBO by varying the amplitude A of the signal. The variation of A will vary the value of the variance σ^2. A perfect channel estimate was considered for simulations.

4.5 Equivalent Rapp Model Parameters

It has already been established that the behavior of millimeter wave power amplifiers are modeled using the modified Bessel-Fourier series model [34]. At present, simulation packages like SIMULINK® do not model millimeter wave power amplifiers. Hence, analysis of millimeter wave systems in these packages need to be done by fitting the modified Bessel-Fourier series model to existing models present in these packages. Since, the Rapp model is the most commonly used model for SSPAs, a methodology to evaluate the equivalent parameters for the

Rapp model for modeling a millimeter wave power amplifiers in current simulation packages is derived in this section. By deriving these equivalent parameters, the analysis of millimeter wave power amplifiers can be carried out in current simulation packages by merely substituting the parameter values rather than coding and simulating the entire modified Bessel-Fourier series model.

The equivalent Rapp model parameters to model a millimeter wave power amplifier is an approximation model and small deviations will still exist to the actual millimeter wave systems. Nonetheless, the parameters can be applied to existing Rapp models in simulation packages to make approximate analysis of millimeter wave power amplifiers.

4.5.1 Parameter Estimation Technique

The Rapp model is given by equation 2.9 which requires the estimate of three parameters namely the linear gain A, saturation level x_0 and the smoothness factor p. In this section, the methodology of deriving the equivalent parameters of the Rapp model is described and the derived parameters are verified to see whether it matches the modified Bessel-Fourier series model of the power amplifier. With the knowledge of these parameters, the inverse Rapp model described in Chapter-3 can be used to compensate millimeter wave signals impaired by power amplifier distortions.

The modified Bessel-Fourier series curve with $\alpha = 0.6$, shown in Fig. 2.14 is considered. Since the Rapp model is described using three parameters, a minimum of three points on the curve are needed for fitting the curve and derive the parameters. The three points can be considered, each at 10%, 50% and 90%, and corresponding input power and output powers at these points are noted. The least squares curve fitting method can be used to fit the Rapp model

to these three points. Here two methods are described to estimate these parameters; one is the least squares technique and in the second method, an analytical expression is derived which uses the information of the three points to estimate the parameters.

4.5.2 Least Squares Curve Fitting

The least squares curve fitting is one of the most commonly used technique for fitting curves to a known function. It is a minimization problem considering a number of data points to fit a curve. Given the output of the power amplifier as $\tilde{x}[n]$ with P number of points on the curve, the least squares curve fitting is done by solving the minimization problem in (4.31) for the parameters A, x_0 and p of the power amplifier. This method is capable of making a good approximation for the parameters of the Rapp model and the accuracy is higher with more data points. A minimum of 3 points are required to estimate these parameters.

$$\arg\min_{A,x_0,p} Err = \arg\min_{A,x_0,p} \sum_{i=1}^{P} \left(\tilde{x}_i[n] - \frac{A x_i[n]}{\left[1 + \left(\frac{A x_i[n]}{x_0}\right)^{2p}\right]^{\frac{1}{2p}}} \right)^2 \tag{4.31}$$

It is found that the ideal points to be considered are at 10, 50 and 90% for the least squares estimation nonetheless better estimates are obtained for higher number of points.

With the motive of arriving at a better estimate with the least number of data points, another analytical expression has been derived for this purpose. This method also reduces the calculation time and complexity of the estimation process, and can be efficiently used for the parameter estimation.

4.5.3 Analytical Expression for Estimation of Parameters

In this section, a closed form expression in terms of the three input and output data points on the modified Bessel-Fourier series power amplifier model output characteritics curve has been derived to calculate the equivalent Rapp model parameters namely the linear gain A, smoothness factor p and saturation level x_0.

Let the input points in the MBF series model curve of Fig. 2.14 be denoted as (x_1, x_2, x_3) and the respective output points be denoted as $(\tilde{x}_1, \tilde{x}_2, \tilde{x}_3)$, where $\tilde{x}_n$ is given by equation 4.7 when an input of magnitude x_n is given to the power amplifier. The relation between these three input and three output points can be expressed using the Rapp model as

$$\tilde{x}_1 = \frac{Ax_1}{\left[1 + \left(\frac{Ax_1}{x_0}\right)^{2p}\right]^{\frac{1}{2p}}} \tag{4.32a}$$

$$\tilde{x}_2 = \frac{Ax_2}{\left[1 + \left(\frac{Ax_2}{x_0}\right)^{2p}\right]^{\frac{1}{2p}}} \tag{4.32b}$$

$$\tilde{x}_3 = \frac{Ax_3}{\left[1 + \left(\frac{Ax_3}{x_0}\right)^{2p}\right]^{\frac{1}{2p}}} \tag{4.32c}$$

Rearranging equation 4.32a and solving for A

$$A = \frac{\tilde{x}_1}{x_1}\left[\frac{1}{1 - \left(\frac{\tilde{x}_1}{x_0}\right)^{2p}}\right]^{\frac{1}{2p}} \tag{4.33}$$

Substituting for A in equation 4.32b from equation 4.33 (Ref. Appendix A),

$$x_0 = \left[\frac{(\tilde{x}_1\tilde{x}_2)^{2p}(x_2^{2p} - x_1^{2p})}{(\tilde{x}_1 x_2)^{2p} - (\tilde{x}_2 x_1)^{2p}}\right]^{\frac{1}{2p}} \tag{4.34}$$

Both equation 4.33 and equation 4.34 require the information of the value of p for estimating A and x_0. Thus, substituting for A and x_0 in equation 4.32c and simplifying further (Ref. Appendix A),

$$\begin{aligned}(x_1x_2\tilde{x}_2\tilde{x}_3)^{2p} - (x_1x_2\tilde{x}_1\tilde{x}_3)^{2p} + (x_2x_3\tilde{x}_1\tilde{x}_3)^{2p} - (x_1x_3\tilde{x}_2\tilde{x}_3)^{2p} \\ +(x_1x_3\tilde{x}_1\tilde{x}_2)^{2p} - (x_2x_3\tilde{x}_1\tilde{x}_2)^{2p} = 0\end{aligned} \tag{4.35}$$

The estimated p is later used in equation 4.33 and equation 4.34 to estimate A and x_0 parameters of the power amplifier.

4.5.4 Calculation and Results

To test the analytical expression derived for estimating the parameters, the modified Bessel-Fourier series model implemented in this chapter for millimeter wave power amplifier distortion analysis was considered as an example. In order to estimate the parameters using equation 4.33, equation 4.34 and equation 4.35, three points at $10\%, 50\%$ and 90% of the values were considered. From the normalized output characteristics, the points at $x_1 = 0.1$, $x_2 = 0.5$ and $x_3 = 0.9$ were considered. The corresponding values of $\tilde{x}$ were $\tilde{x}_1 = 0.2011$, $\tilde{x}_2 = 0.8567$ and $\tilde{x}_3 = 1.0604$ respectively. Using these values in equation 4.32, three nonlinear equations with three unknowns are obtained. Simplifying and solving using equation 4.33, equation 4.34 and equation 4.35, the parameters for a LDMOS power amplifier considered in this chapter for

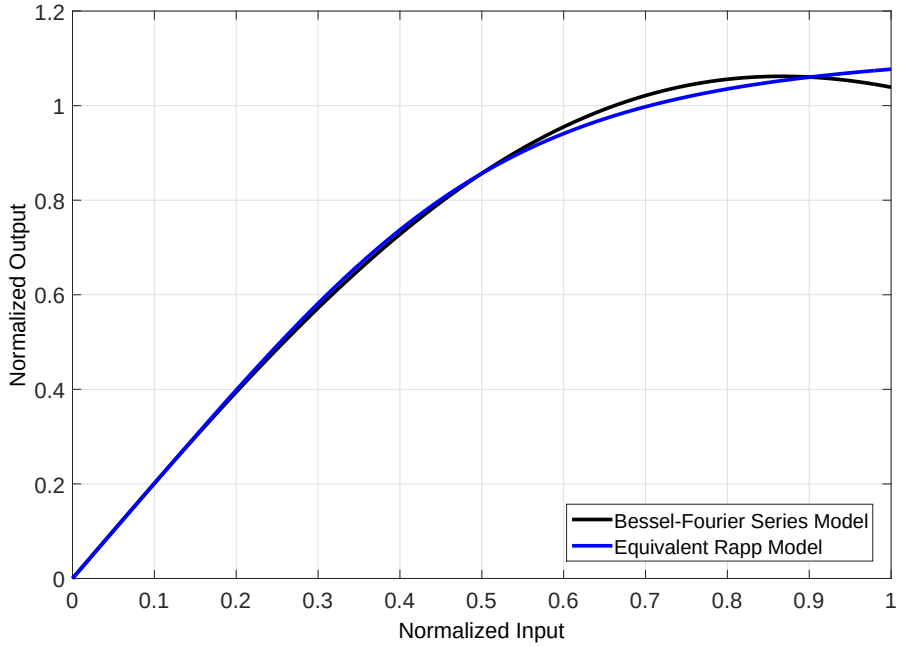

Figure 4.4: Equivalent Rapp Model for Millimeter wave Power Amplifier

simulations were estimated as $p = 1.641$, $A = 2.013$ and $x_0 = 1.123$.

In order to verify the validity of the estimated parameters, these values were substituted in the Rapp model and the output characteristics were plotted in comparison to the modified Bessel-Fourier series and are as shown in Fig. 4.4. It was found that the Rapp model using the extracted parameters closely match that of the modified Bessel-Fourier series curve.

4.6 Summary

This chapter talks about a simplified model for the analysis of a millimeter wave OFDM system impaired by nonlinear distortions. An analytical expression has been derived for the calculation of the symbol error probability for an OFDM system with nonlinear distortions. A method for deriving the equivalent Rapp model parameters for the modified Bessel-Fourier series model of

the power amplifier is given and shown that these parameters match the output characteristics for the modified Bessel-Fourier series model. This analysis can be helpful for evaluating the performance of 5G OFDM systems theoretically instead of performing complex simulations and develop receiver end compensation models for nonlinear distortions.

Chapter 5

Conclusions and Future Work

5.1 Contributions of the Thesis

Two main contributions are made in this thesis which has the scope of potential future work. The contributions are discussed as follows

A two-step pilot signal based power amplifier nonlinear distortion compensator for a MIMO-STBC (Multiple Input Multiple Output-Space Time Block Code) system modulated by a QAM (Quadrature Amplitude Modulation) wireless communication systems is designed. In the proposed method, a methodology to identify the source of distortion, its compensation and application in a transmitter device identification process is proposed using a two-step pilot signal approach. Step one involves the estimation of the channel and the step two estimates the transmitter parameters which are used to compensate distortions and identify the device. The device identification process involves the comparison of the estimated transmitter device parameters with a validated set of parameters. Results from computer simulation show that the proposed compensation method has a significantly good performance in terms of the bit error rate of the system and successfully identifies the transmitter device. The proposed methodology decreases the complexity of the receiver signal processing for distortion compensation since the parame-

ters for the power amplifier distortion compensator are estimated once, it can be subsequently used for all data symbols without re-estimation.

With the millimeter wave signals gaining importance in today's communication systems, it is essential to study their behavior and performance when subject to various distortions. That being considered, the performance of a millimeter wave Orthogonal Frequency Division Multiplexing (OFDM) wireless communication system in presence of power amplifier nonlinear distortions is studied and an analytical expression for the symbol error probability has been derived. The results of the analytical expression is compared to values of a computer simulated communication system and verified. This analytical expression enables the study of the performance of OFDM systems theoretically, thus avoiding complex simulations to estimate the performance of millimeter wave systems. A procedure to obtain the equivalent Rapp model parameters is also proposed for millimeter wave power amplifiers.

5.2 Future Prospects

Power amplifier analysis have been carried out in this thesis considering only the amplitude (AM-AM) nonlinear distortions. Both the Rapp model and modified Bessel-Fourier series model do not consider the phase nonlinearities which may exist in real-time power amplifiers. These phase distortions may effect the quality of signals in communication systems and hence, analysis of such systems may be considered depending on the severity and applicability of these distortions.

The systems implemented in this thesis assumes a perfect channel estimate and thus the analysis results were based on only the power amplifier distortions. Chances of a varied performance exist when an imperfect channel estimate occurs and analysis need to carried out in

this direction.

The nonlinear compensator proposed in Chapter 3 uses an inverse Rapp model to perform the compensation which is a nonlinear model. Works on realizing such nonlinear models as a transmitter end pre-distorter device into circuits exist [54]. On similar lines, research activities need to be carried out to develop these models on the receiver end to realize the proposed compensator into hardware circuitry.

With the proposed nonlinear distortion compensation and device identification technique in Chapter 3, the process can be collaborated with other device identification and authentication techniques for enhanced communication security applications to have a secured device-to-device communication. Also, the work can be extended for multiple transmitter - multiple receiver systems by implementing tests like the statistical Welch test for transmitter identification.

The results in Chapter 4 can be used to carry out theoretical analysis on millimeter wave systems impaired by power amplifiers operating at different values of the parameters α, N, c_1 and c_2. The information from the derived Rapp model parameters can be used to study and analyze millimeter wave power amplifiers and design power amplifier nonlinear distortion compensators.

Bibliography

[1] P.K. Bondyopadhyay. "Guglielmo Marconi - The Father of Long Distance Radio Communication - An Engineer's Tribute". In *Microwave Conference, 1995. 25th European*, volume 2, pages 879–885, Sept 1995.

[2] I-Wei Lai Tzi-Dar Chiueh, Pei-Yun Tsai. *"Baseband Receiver Design for Wireless MIMO-OFDM Communications"*. John Wiley and Sons Singapore Pte. Ltd, 2 edition, 2012.

[3] M. Shabany and P.G. Gulak. "Efficient Compensation of the Nonlinearity of Solid-State Power Amplifiers Using Adaptive Sequential Monte Carlo Methods". *Circuits and Systems I: Regular Papers, IEEE Transactions on*, 55(10):3270–3283, Nov 2008.

[4] R. Achar and M.S. Nakhla. "Simulation of High-speed Interconnects". *Proceedings of the IEEE*, 89(5):693–728, May 2001.

[5] Lili Wei, R. Hu, Yi Qian, and Geng Wu. "Key Elements to Enable Millimeter Wave Communications for 5G Wireless Systems". *Wireless Communications, IEEE*, 21(6):136–143, December 2014.

[6] A.J. Paulraj, D.A. GORE, R.U. Nabar, and H. Bolcskei. "An Overview of MIMO Communications - A key to Gigabit Wireless". *Proceedings of the IEEE*, 92(2):198–218, Feb 2004.

[7] Vahid Tarokh, Hamid Jafarkhani, and A.R. Calderbank. "Space-time Block Coding for Wireless Communications: Performance Results". *Selected Areas in Communications, IEEE Journal on*, 17(3):451–460, Mar 1999.

[8] Taewon Hwang, Chenyang Yang, Gang Wu, Shaoqian Li, and G.Y. Li. "OFDM and Its Wireless Applications: A Survey". *Vehicular Technology, IEEE Transactions on*, 58(4):1673–1694, May 2009.

[9] V.A. Bohara and S.H. Ting. "Analytical Performance of Orthogonal Frequency Division Multiplexing Systems Impaired by a Non-linear high-power Amplifier with Memory". *Communications, IET*, 3(10):1659–1666, October 2009.

[10] Hao. Li. *"Physical-Layer Security Enhancement in Wireless Communication Systems"*. MESc Thesis, Electronic Thesis and Dissertation Repository, University of Western Ontario, London, Canada, 2013.

[11] Adel S. Sedra and Kenneth C. Smith. *"Microelectronic Circuits Revised Edition"*. Oxford University Press, Inc., New York, NY, USA, 6th edition, 2009.

[12] Peng Hao, Xianbin Wang, and A. Behnad. "Performance Enhancement of I/Q Imbalance based Wireless Device Authentication Through Collaboration of Multiple Receivers". In *Communications (ICC), 2014 IEEE International Conference on*, pages 939–944, June 2014.

[13] Shaodan Ma and Tung-Sang Ng. "Semi-Blind Time-Domain Equalization for MIMO-OFDM Systems". *Vehicular Technology, IEEE Transactions on*, 57(4):2219–2227, July 2008.

[14] Paulo Sergio Diniz. *"Adaptive Filtering: Algorithms and Practical Implementation"*. Kluwer Academic Publishers, Norwell, MA, USA, 2 edition, 2002.

[15] W.R. Wu, C.F. Lee, and Y.F. Chen. "Time-domain Equalisation for Discrete Multitone Transceivers: New Results and Performance Analysis". *Communications, IET*, 3(7):1186–1200, July 2009.

[16] P. Drotar, J. Gazda, M. Deumal, P. Galajda, and D. Kocur. "Receiver based Compensation of Nonlinear Distortion in MIMO-OFDM". In *RF Front-ends for Software Defined and Cognitive Radio Solutions (IMWS), 2010 IEEE International Microwave Workshop Series on*, pages 1–4, Feb 2010.

[17] Jian Qi and S. Aissa. "Analysis and Compensation of Power Amplifier Nonlinearity in MIMO Transmit Diversity Systems". *Vehicular Technology, IEEE Transactions on*, 59(6):2921–2931, July 2010.

[18] F. Gregorio, S. Werner, T.I. Laakso, and J. Cousseau. "Receiver Cancellation Technique for Nonlinear Power Amplifier Distortion in SDMA-OFDM Systems". *Vehicular Technology, IEEE Transactions on*, 56(5):2499–2516, Sept 2007.

[19] F.H. Gregorio, S. Werner, J.E. Cousseau, and R. Wichman. "Broadband Power Amplifier Distortion Cancellation with Model Estimation in the Receiver". In *Signal Processing Advances in Wireless Communications, 2007. SPAWC 2007. IEEE 8th Workshop on*, pages 1–5, June 2007.

[20] Ishtiaq Ahmad, Ahmed Iyanda Sulyman, Abdulhameed Alsanie, Awad Kh Alasmari, and Saleh Alshebeili. "Spectral Broadening Effects of High Power Amplifiers in MIMO-OFDM Relaying Channels". *EURASIP Journal on Wireless Communications and Networking*, 2013(1):32, 2013.

[21] A.A.M. Saleh. “Frequency-Independent and Frequency-Dependent Nonlinear Models of TWT Amplifiers”. *Communications, IEEE Transactions on*, 29(11):1715–1720, November 1981.

[22] C. Rapp. “Effects of HPA-Nonlinearity on a 4-DPSK/OFDM-Signal for a Digital Sound Broadcasting System”. In *Proceedings of the Second European Conference on Satellite Communication*, pages 179–184, Oct 1991.

[23] J.W. Craig. “A New, Simple and Exact Result for Calculating the Probability of Error for two-dimensional Signal Constellations”. In *Military Communications Conference, 1991. MILCOM ’91, Conference Record, Military Communications in a Changing World., IEEE*, pages 571–575 vol.2, Nov 1991.

[24] Peter Jantunen. *“Modelling of Nonlinear Power Amplifiers for Wireless Communication”*. Master’s Thesis, Helsinki University of Technology, Espoo, Finland, 2004.

[25] R. Raich, Hua Qian, and G.T. Zhou. “Orthogonal Polynomials for Power Amplifier Modeling and Predistorter Design”. *Vehicular Technology, IEEE Transactions on*, 53(5):1468–1479, Sept 2004.

[26] MATLAB Documentation. *“Apply Memoryless Nonlinearity to Complex Baseband Signal”*. MathWorks.

[27] M. O’Droma, S. Meza, and Yiming Lei. “New Modified Saleh Models for Memoryless Nonlinear Power Amplifier Behavioural Modelling”. *Communications Letters, IEEE*, 13(6):399–401, June 2009.

[28] Michel Allegue-Martnez, Mara J. Madero-Ayora, Carlos Crespo-Cadenas, Javier Reina-Tosina, and Francisco Bernardo. “Nonlinear Effects in LTE Downlink Signals and Application of a Compensation Technique at the Receiver side”. *Microwave and Optical Technology Letters*, 54(1):54–58, 2012.

[29] Hanen Bouhadda, Hmaied Shaiek, Daniel Roviras, Rafik Zayani, Yahia Medjahdi, and Ridha Bouallegue. “Theoretical Analysis of BER Performance of Nonlinearly Amplified FBMC/OQAM and OFDM signals”. *EURASIP Journal on Advances in Signal Processing*, 2014(1):60, 2014.

[30] T. Vuolevi, J. Rahkonen. *“Distortion in RF Power Amplifiers”*. Norwood, MA: Artech House,, 2003.

[31] E.W. Bai, V. Cerone, and D. Regruto. “Separable Inputs for the Identification of Block-oriented Nonlinear Systems”. In *American Control Conference, 2007. ACC ’07*, pages 1548–1553, July 2007.

[32] J.C. Pedro, N.B. Carvalho, and P.M. Lavrador. "Modeling Nonlinear Behavior of Band-pass Memoryless and Dynamic Systems". In *Microwave Symposium Digest, 2003 IEEE MTT-S International*, volume 3, pages 2133–2136 vol.3, June 2003.

[33] J.C. Pedro and S.A. Maas. "A Comparative Overview of Microwave and Wireless Power Amplifier Behavioral Modeling Approaches". *Microwave Theory and Techniques, IEEE Transactions on*, 53(4):1150–1163, April 2005.

[34] Luca Roselli. Apostolos Georgiadis, Hendrik Rogier and Paolo Arcioni. *"Microwave and Millimeter Wave Circuits and Systems: Emerging Design, Technologies, and Applications"*. John Wiley and Sons, Ltd,, 1 edition, 2013.

[35] M.S. O'Droma. "Dynamic Range and other Fundamentals of the Complex Bessel Function Series Approximation Model for Memoryless Nonlinear Devices". *Communications, IEEE Transactions on*, 37(4):397–398, Apr 1989.

[36] M. O'Droma and Yiming Lei. "A Novel Optimization Method for Nonlinear Bessel-Fourier PA Model Using an Adjusted Instantaneous Voltage Transfer Characteristic". In *Microwave Conference, 2008. EuMC 2008. 38th European*, pages 1269–1272, Oct 2008.

[37] M. O'droma and Lei Yiming. "A New Bessel-Fourier Memoryless Nonlinear Power Amplifier Behavioral Model". *Microwave and Wireless Components Letters, IEEE*, 23(1):25–27, Jan 2013.

[38] Xuyen Vuong and H. Moody. "Comment on 'A General Theory for Intelligible Crosstalk Between Frequency-Division Multiplexed Angle-Modulated Carriers'". *Communications, IEEE Transactions on*, 28(11):1939–1943, November 1980.

[39] Xuyen Vuong and M. Henchey. "On the Accuracy of the Shimbo Approach to Intermodulation and Crosstalk Calculations". *Communications, IEEE Transactions on*, 29(7):1076–1082, Jul 1981.

[40] O. Shimbo and L.N. Nguyen. "Further Clarification on the Use of Bessel Function Expansion to Approximate TWTA Nonlinear Characteristics". *Communications, IEEE Transactions on*, 30(2):418–419, Feb 1982.

[41] Raman K. Attri. "Practical Design Evaluation of Extremely Narrow Band-Pass Filter Topologies". *Instrumentation Design Series (Electronics)*, September 2005.

[42] P.L. Gilabert, A. Cesari, G. Montoro, E. Bertran, and J.-M. Dilhac. "Multi-Lookup Table FPGA Implementation of an Adaptive Digital Predistorter for Linearizing RF Power Amplifiers With Memory Effects". *Microwave Theory and Techniques, IEEE Transactions on*, 56(2):372–384, Feb 2008.

[43] F.H. Gregorio. *"Analysis and Compensation of Nonlinear Power Amplifier Effects in Multi-antenna OFDM Systems"*. PhD Dissertation, Helsinki University of Technology, Espoo, Finland, 2007.

[44] Boris Danev, Davide Zanetti, and Srdjan Capkun. "On Physical-Layer Identification of Wireless Devices". *ACM Comput. Surv.*, 45(1):6:1–6:29, December 2012.

[45] Nam Tuan Nguyen, Guanbo Zheng, Zhu Han, and Rong Zheng. "Device Fingerprinting to Enhance Wireless Security using Nonparametric Bayesian Method". In *INFOCOM, 2011 Proceedings IEEE*, pages 1404–1412, April 2011.

[46] D.C. Montgomery, G.C. Runger, and N.F. Hubele. *"Engineering Statistics"*. Wiley, 2010.

[47] E. Perahia. "IEEE P802.11 Wireless LANs TGad Evaluation Methodology". Technical report, September 2010.

[48] Mark Webster. "Suggested PA Model for 802.11 HRb". Technical report, September 2000.

[49] C. Dehos and T.C.W. Schenk. "Digital Compensation of Amplifier Nonlinearities in the Receiver of a Wireless System". In *Communications and Vehicular Technology in the Benelux, 2007 14th IEEE Symposium on*, pages 1–6, Nov 2007.

[50] V.A. Bohara and See Ho Ting. "Theoretical Analysis of OFDM Signals in Nonlinear Polynomial Models". In *Information, Communications Signal Processing, 2007 6th International Conference on*, pages 1–5, Dec 2007.

[51] V.A. Bohara and See Ho Ting. "Analysis of OFDM Signals in Nonlinear High Power Amplifier with Memory". In *Communications, 2008. ICC '08. IEEE International Conference on*, pages 3653–3657, May 2008.

[52] I.S. Gradshteyn and I.M. Ryzhik. *"Table of Integrals, Series, and Products"*, pages 959–960. New York Academic.

[53] J.G. Proakis and M. Salehi. *"Digital Communication"*. Kluwer Academic Publishers, 2004.

[54] Ylva Jung. *Estimation of Inverse Models Applied to Power Amplifier Predistortion*. Linkping Studies in Science and Technology. Thesis, Linkping UniversityLinkping University, Automatic Control, The Institute of Technology, 2013.

Appendix A

Appendix

A.1 Received Signal Representation

Equation 4.11 is

$$\begin{aligned} Y_m &= \sum_{l=1}^{L} h_l\left(\frac{\alpha c_1}{2}\right)\sum_{n=0}^{N-1} x[n]e^{-\frac{j2\pi mn}{N}}e^{-\frac{j2\pi m\tau_l}{N}} \\ &\quad + \sum_{l=1}^{L} h_l\left(\frac{-\alpha c_2}{2}\right)\sum_{n=0}^{N-1} x[n]|x[n]|^2 e^{-\frac{j2\pi mn}{N}}e^{-\frac{j2\pi m\tau_l}{N}} + w_l[m] \\ &= \delta + \Delta + w_l \end{aligned} \tag{A.1}$$

Consider Δ and expanding the summation [9],

$$\Delta = \sum_{l=1}^{L} h_l\left(\frac{-\alpha c_2}{2}\right)\Bigg(x[0]|x[0]|^2 + x[1]|x[1]|^2 e^{-\frac{j2\pi m}{N}} + \ldots + x[N-1]|x[N-1]|^2 e^{-\frac{j2\pi m(N-1)}{N}}\Bigg)e^{-\frac{j2\pi m\tau_l}{N}}$$

Expressing $|x[n]|^2 = \gamma_n$, taking IDFT and simplifying,

$$\begin{aligned}\Delta &= \sum_{l=1}^{L} h_l\left(\frac{-\alpha c_2}{2N}\right)\left\{\gamma_0\sum_{q_1=0}^{N-1}X_{q_1} + \gamma_1 e^{-\frac{j2\pi m}{N}}\sum_{q_1=0}^{N-1}X_{q_1}e^{\frac{j2\pi q_1}{N}} + \gamma_2 e^{\frac{-j2\pi m(2)}{N}}\sum_{q_1=0}^{N-1}X_{q_1}e^{\frac{j2\pi q_1(2)}{N}}\right.\\ &\left. + \cdots + \gamma_{N-1}e^{-\frac{j2\pi m(N-1)}{N}}\sum_{q_1=0}^{N-1}X_{q_1}e^{\frac{j2\pi q_1(N-1)}{N}}\right\}e^{\frac{-j2\pi m\tau_l}{N}}\\ &= \sum_{l=1}^{L} h_l\left(\frac{-\alpha c_2}{2N}\right)\left\{\sum_{n=0}^{N-1}\gamma_n e^{-\frac{j2\pi mn}{N}}\sum_{q_1=0}^{N-1}X_{q_1}e^{\frac{j2\pi q_1 n}{N}}\right\}e^{-\frac{j2\pi m\tau_l}{N}}\end{aligned} \tag{A.2}$$

Consolidating X_m terms in equation A.2, equation 4.12 is obtained.

A.2 Expected Values of $\sum_{n=0}^{N-1}\gamma_n$ and $\sum_{n=0}^{N-1}\gamma_n^2$

The expected value of $\sum_{n=0}^{N-1}\gamma_n$ is derived as follows

$$\begin{aligned}E\left[\sum_{n=0}^{N-1}\gamma_n\right] &= E\left[\sum_{n=0}^{N-1}\left|x[n]\right|^2\right] = \sum_{n=0}^{N-1}E\left[\left|x[n]\right|^2\right] = \sum_{n=0}^{N-1}\sum_{m_1=0}^{N-1}\sum_{m_2=0}^{N-1}\frac{E\left[X_{m_1}X_{m_2}^*\right]}{N^2}e^{\frac{j2\pi(m_1-m_2)n}{N}}\\ &= \begin{cases}\sum_{n=0}^{N-1}\sum_{m_1=0}^{N-1}\frac{E[|X_{m_1}|^2]}{N^2} & \text{if } m_1{=}m_2\\ 0 & \text{otherwise}\end{cases}\\ &= \frac{N^2\sigma^2}{N^2} = \sigma^2\end{aligned} \tag{A.3}$$

The expected value of $\sum_{n=0}^{N-1} \gamma_n^2$ is derived as follows. Consider

$$\begin{aligned} \gamma_n.\gamma_m &= |x[n]|^2.|x[m]|^2 \\ &= \frac{1}{N^4} \sum_{p=0}^{N-1} \sum_{q=0}^{N-1} \sum_{r=0}^{N-1} \sum_{s=0}^{N-1} X_p X_q^* X_r X_s^* e^{\frac{j2\pi(p-q)n}{N}} e^{\frac{j2\pi(r-s)m}{N}} \end{aligned} \tag{A.4}$$

Taking expectation on both sides,

$$E\left[|x[n]|^2|x[m]|^2\right] = \frac{1}{N^4} \sum_{p=0}^{N-1} \sum_{q=0}^{N-1} \sum_{r=0}^{N-1} \sum_{s=0}^{N-1} E\left[X_p X_q^* X_r X_s^*\right] e^{\frac{j2\pi(p-q)n}{N}} e^{\frac{j2\pi(r-s)m}{N}} \tag{A.5}$$

When $p = q = r = s$,

$$\begin{aligned} E\left[X_p X_q^* X_r X_s^*\right] &= E[|X_p|^4] = E[(|X_p|^2)^2] \\ &= E[(X_{p_{Re}}^2 + X_{p_{Im}}^2)^2] \\ &= E[X_{p_{Re}}^4 + X_{p_{Im}}^4 + 2X_{p_{Re}}^2 X_{p_{Im}}^2] \\ &= 3\left(\frac{\sigma^2}{2}\right)^2 + 3\left(\frac{\sigma^2}{2}\right)^2 + \frac{(\sigma^2)^2}{2} = \frac{7(\sigma^2)^2}{2} \end{aligned} \tag{A.6}$$

where *Re* and *Im* denote the real and imaginary parts of X_p. When $p = q \neq r = s$ or $p = s \neq q = r$,

$$E\left[X_p X_q^* X_r X_s^*\right] = E[|X_p|^2|X_r|^2] = (\sigma^2)^2 \tag{A.7}$$

Using these values of expectation in equation A.5 with $n = m$ and simplifying,

$$\begin{aligned} E\left[\left(\sum_{n=0}^{N-1}\gamma_n\right)^2\right] &= \sum_{n=0}^{N-1}\sum_{n=0}^{N-1} E\left[(\gamma_n)^2\right] \\ &= N^2\left[\frac{1}{N^4}\left(\frac{7N(\sigma^2)^2}{2} + (N^2-N)(\sigma^2)^2\right)\right] \\ &= (\sigma^2)^2\left(1+\frac{5}{2N}\right) \approxeq (\sigma^2)^2 \because \text{N is large} \end{aligned} \tag{A.8}$$

A.3 Equivalent Rapp Model Parameters

A.3.1 Estimation of Saturation Level 'x_0'

We have from equation 4.33,

$$\boxed{\hat{A} = \frac{\tilde{x}_1}{x_1}\left[\frac{1}{1-(\frac{\tilde{x}_1}{x_0})^{2p}}\right]^{\frac{1}{2p}}} \tag{A.9}$$

Substituting equation 4.33 in equation 4.32b in place of A,

$$\tilde{x}_2 = \frac{\tilde{x}_1}{x_1}\left[\frac{1}{1-(\frac{\tilde{x}_1}{x_0})^{2p}}\right]^{\frac{1}{2p}} x_2 \Bigg/ \left[1+\left(\frac{\tilde{x}_1}{x_1}\left[\frac{1}{1-(\frac{\tilde{x}_1}{x_0})^{2p}}\right]^{\frac{1}{2p}} x_2/x_0\right)^{2p}\right]^{\frac{1}{2p}} \tag{A.10}$$

Raising the LHS and RHS to the power of $2p$ and simplifying,

$$\tilde{x}_2^{2p} = \left[\frac{\tilde{x}_1 x_2}{x_1}\right]^{2p}\left[\frac{1}{1-(\frac{\tilde{x}_1}{x_0})^{2p}}\right] \Bigg/ \left[1+\left(\frac{\tilde{x}_1 {x_2}^{2p}}{x_1^{2p}x_0^{2p}}\left[\frac{1}{1-(\frac{\tilde{x}_1}{x_0})^{2p}}\right]\right)\right]$$

Cross multiplying,

$$\tilde{x}_2^{2p}\left[1-\left(\frac{\tilde{x}_1}{x_0}\right)^{2p}\right]\left[1+\left(\frac{\tilde{x}_1 {x_2}^{2p}}{x_1^{2p}x_0^{2p}}\left[\frac{1}{1-(\frac{\tilde{x}_1}{x_0})^{2p}}\right]\right)\right]=\left[\frac{\tilde{x}_1 x_2}{x_1}\right]^{2p}$$

Multiplying the two bracket terms in LHS, and simplifying

$$\begin{aligned}
&\tilde{x}_2^{2p}\left[1-\left(\frac{\tilde{x}_1}{x_0}\right)^{2p}+\frac{\tilde{x}_1 {x_2}^{2p}}{x_1^{2p}x_0^{2p}}\right]=\left[\frac{\tilde{x}_1 x_2}{x_1}\right]^{2p}\\
&\tilde{x}_2^{2p}+\frac{\tilde{x}_2^{2p}}{x_0^{2p}}\left[\left(\frac{\tilde{x}_1 x_2}{x_1}\right)^{2p}-x_1^{2p}\right]=\left[\frac{\tilde{x}_1 x_2}{x_1}\right]^{2p}\\
&\frac{\tilde{x}_2^{2p}}{x_0^{2p}}\left[\left(\frac{\tilde{x}_1 x_2}{x_1}\right)^{2p}-x_1^{2p}\right]=\left[\frac{\tilde{x}_1 x_2}{x_1}\right]^{2p}-\tilde{x}_2^{2p}\\
&\frac{(\tilde{x}_2\tilde{x}_1 x_2)^{2p}-(\tilde{x}_1\tilde{x}_2 x_1)^{2p}}{x_0^{2p}}=(\tilde{x}_1 x_2)^{2p}-(\tilde{x}_2 x_1)^{2p}
\end{aligned}$$

Simplifying this, rearranging and taking out $\tilde{x}_1\tilde{x}_2$ common in the last step,

$$\boxed{\hat{x}_0=\left[\frac{(\tilde{x}_1\tilde{x}_2)^{2p}(x_2^{2p}-x_1^{2p})}{(\tilde{x}_1 x_2)^{2p}-(\tilde{x}_2 x_1)^{2p}}\right]^{\frac{1}{2p}}} \tag{A.11}$$

A.3.2 Estimation of Smoothness Factor 'p'

From equation 4.32c,

$$\tilde{x}_3=\frac{Ax_3}{\left[1+\left(\frac{Ax_3}{x_0}\right)^{2p}\right]^{\frac{1}{2p}}} \tag{A.12}$$

Raising the LHS and RHS to the power of $2p$ and simplifying,

$$\tilde{x}_3^{2p} = \frac{(Ax_3)^{2p}}{\left[1 + \left(\frac{Ax_3}{x_0}\right)^{2p}\right]} \tag{A.13}$$

Substituting for A with the estimate $\hat{A}$ from equation 4.33 in the above equation and simplifying,

$$\begin{aligned}
\tilde{x}_3^{2p} &= \frac{\left(\frac{\tilde{x}_1}{x_1}\right)^{2p}\left[\frac{1}{1-\left(\frac{\tilde{x}_1}{x_0}\right)^{2p}}\right]x_3^{2p}}{1 + \left(\frac{\frac{\tilde{x}_1}{x_1}\left[\frac{1}{1-\left(\frac{\tilde{x}_1}{x_0}\right)^{2p}}\right]^{\frac{1}{2p}} x_3}{x_0}\right)^{2p}} \\
&= \left(\frac{\tilde{x}_1 x_3}{x_1}\right)^{2p} \frac{\left[\frac{1}{1-\left(\frac{\tilde{x}_1}{x_0}\right)^{2p}}\right]}{1 + \left(\left(\frac{\tilde{x}_1 x_3}{x_1 x_0}\right)^{2p}\left[\frac{1}{1-\left(\frac{\tilde{x}_1}{x_0}\right)^{2p}}\right]\right)}
\end{aligned} \tag{A.14}$$

$$\tilde{x}_3^{2p} = \left(\frac{\tilde{x}_1 x_3}{x_1}\right)^{2p} \frac{\left[\frac{1}{1-\left(\frac{\tilde{x}_1}{x_0}\right)^{2p}}\right]}{1 + D} \tag{A.15}$$

where $D = \left(\left(\frac{\tilde{x}_1 x_3}{x_1 x_0}\right)^{2p}\left[\frac{1}{1-\left(\frac{\tilde{x}_1}{x_0}\right)^{2p}}\right]\right)$.

D is calculated before so that it is easier to simplify. Substituting for x_0 in equation A.15,

$$D = \left(\frac{\tilde{x}_1 x_3}{x_1 \left[\frac{(\tilde{x}_1\tilde{x}_2)^{2p}(x_2^{2p}-x_1^{2p})}{(\tilde{x}_1 x_2)^{2p}-(\tilde{x}_2 x_1)^{2p}} \right]^{\frac{1}{2p}}} \right)^{2p} \left[\frac{1}{1 - \left(\frac{\tilde{x}_1}{\left[\frac{(\tilde{x}_1\tilde{x}_2)^{2p}(x_2^{2p}-x_1^{2p})}{(\tilde{x}_1 x_2)^{2p}-(\tilde{x}_2 x_1)^{2p}} \right]^{\frac{1}{2p}}} \right)^{2p}} \right] \tag{A.16}$$

$$= \left(\frac{\tilde{x}_1 x_3}{x_1} \right)^{2p} \frac{1}{\left(\frac{(\tilde{x}_1\tilde{x}_2)^{2p}(x_2^{2p}-x_1^{2p})}{(\tilde{x}_1 x_2)^{2p}-(\tilde{x}_2 x_1)^{2p}} \right) \left(1 - \left(\frac{\tilde{x}_1^{2p}\left((\tilde{x}_1 x_2)^{2p}-(\tilde{x}_2 x_1)^{2p}\right)}{(\tilde{x}_1\tilde{x}_2)^{2p}(x_2^{2p}-|s_1|^{2p})} \right)^{2p} \right)} \tag{A.17}$$

$$= \left(\frac{\tilde{x}_1 x_3}{x_1} \right)^{2p} \frac{1}{\left[\frac{(\tilde{x}_1\tilde{x}_2)^{2p}(x_2^{2p}-x_1^{2p})}{(\tilde{x}_1 x_2)^{2p}-(\tilde{x}_2 x_1)^{2p}} \right] \left(1 - \left(\frac{\left((\tilde{x}_1 x_2)^{2p}-(\tilde{x}_2 x_1)^{2p}\right)}{(\tilde{x}_2)^{2p}(x_2^{2p}-x_1^{2p})} \right)^{2p} \right)}$$

$$D = \left(\frac{\tilde{x}_1 x_3}{x_1} \right)^{2p} \mathrm{X} \tag{A.18}$$

$$\frac{(\tilde{x}_2)^{2p}(x_2^{2p} - x_1^{2p})\left((\tilde{x}_1 x_2)^{2p} - (\tilde{x}_2 x_1)^{2p}\right)}{(\tilde{x}_1\tilde{x}_2)^{2p}(x_2^{2p} - x_1^{2p})\left[\tilde{x}_2 x_2)^{2p} - (\tilde{x}_2 x_1^{2p}) - (\tilde{x}_1 x_2)^{2p} + (\tilde{x}_2 x_1)^{2p}\right]}$$

Two terms in the denominator of equation A.18 gets canceled due to the plus and minus sign, and three terms between the numerator and denominator get canceled. Hence,

$$D = \frac{x_3^{2p}\left((\tilde{x}_1 x_2)^{2p} - (\tilde{x}_2 x_1)^{2p}\right)}{(x_1 x_2)^{2p}\left(\tilde{x}_2^{2p} - \tilde{x}_1^{2p}\right)} \tag{A.19}$$

Substituting for x_0 with its estimate $\hat{x_0}$ from equation 4.34 and the value of D obtained in equation A.19 in equation A.15,

$$\tilde{x}_3^{2p} = \left(\frac{\tilde{x}_1 x_3}{x_1}\right)^{2p} \frac{\left[\frac{1}{1-\left(\frac{\tilde{x}_1}{\left[\frac{(\tilde{x}_1\tilde{x}_2)^{2p}(x_2^{2p}-x_1^{2p})}{(\tilde{x}_1 x_2)^{2p}-(\tilde{x}_2 x_1)^{2p}}\right]^{\frac{1}{2p}}}\right)^{2p}}\right]}{1+\left(\frac{x_3^{2p}\left((\tilde{x}_1 x_2)^{2p}-(\tilde{x}_2 x_1)^{2p}\right)}{(x_1 x_2)^{2p}\left(\tilde{x}_2^{2p}-\tilde{x}_1^{2p}\right)}\right)}$$

$$= \left(\frac{\tilde{x}_1 x_3}{x_1}\right)^{2p} \frac{\left[\frac{1}{1-\left(\frac{\left((\tilde{x}_1 x_2)^{2p}-(\tilde{x}_2 x_1)^{2p}\right)}{\tilde{x}_2^{2p}(x_2^{2p}-x_1^{2p})}\right)}\right]}{\frac{(x_1 x_2)^{2p}\left(\tilde{x}_2^{2p}-\tilde{x}_1^{2p}\right)+x_3^{2p}\left((\tilde{x}_1 x_2)^{2p}-(\tilde{x}_2 x_1)^{2p}\right)}{(x_1 x_2)^{2p}\left(\tilde{x}_2^{2p}-\tilde{x}_1^{2p}\right)}}$$

$$= \left(\frac{\tilde{x}_1 x_3}{x_1}\right)^{2p} \left[\frac{\tilde{x}_2^{2p}(x_2^{2p}-x_1^{2p})}{\tilde{x}_2^{2p}x_2^{2p}-\tilde{x}_2^{2p}x_1^{2p}-\tilde{x}_1^{2p}x_2^{2p}+\tilde{x}_2^{2p}x_1^{2p}}\right] X$$
$$\left[\frac{x_1^{2p}x_2^{2p}\left(\tilde{x}_2^{2p}-\tilde{x}_1^{2p}\right)}{\left(\tilde{x}_2^{2p}-\tilde{x}_1^{2p}\right)\left(\tilde{x}_2^{2p}-\tilde{x}_1^{2p}\right)+x_3^{2p}\left[\left(\tilde{x}_2 x_2^{2p}\right)^{2p}-\left(\tilde{x}_2 x_1^{2p}\right)\right]}\right]$$

$$= \frac{\tilde{x}_1^{2p}\tilde{x}_2^{2p}x_3^{2p}\left(x_2^{2p}-x_1^{2p}\right)x_2^{2p}\left(\tilde{x}_2^{2p}-\tilde{x}_1^{2p}\right)}{\left(\tilde{x}_2^{2p}-\tilde{x}_1^{2p}\right)x_2^{2p}\left[\left(\tilde{x}_2 x_2^{2p}\right)^{2p}-\left(\tilde{x}_2 x_1^{2p}\right)\right]}$$

Simplifying and rearranging,

$$\begin{aligned}&(x_1x_2\tilde{x}_2\tilde{x}_3)^{2p} - (x_1x_2\tilde{x}_1\tilde{x}_3)^{2p}\\ &+(x_2x_3\tilde{x}_1\tilde{x}_3)^{2p} - (x_1x_3\tilde{x}_2\tilde{x}_3)^{2p}\\ &+(x_1x_3\tilde{x}_1\tilde{x}_2)^{2p} - (x_2x_3\tilde{x}_1\tilde{x}_2)^{2p} = 0\end{aligned} \tag{A.20}$$

Solving this equation estimates p which is subsequently used to estimate x_0 and A. This is a nonlinear equation which can be solved by many numerical method techniques.

Curriculum Vitae

Name:	Sharath Manjunath
Post-Secondary Education and Degrees:	The National Institute of Engineering Mysore, Karnataka, India 2006 - 2010 B.E. The University of Western Ontario London, Ontario, Canada 2013 - 2015 M.E.Sc
Honours and Awards:	NSERC CREATE Program in Communications Security, Privacy and Cyberethics, 2013-2015
Related Work	Graduate Teaching Assistant The University of Wester Ontario 2014-2015

Publications:

1. Sharath Manjunath, Aydin Behnad, Xianbin Wang and Anestis Dounavis, "A Two-step Pilot Signal Approach for Distortion Compensation and Transmitter Identification in Wireless Communication Systems", *6th International Conference and Workshop on Computing and Communication*, Oct. 2015

2. Sharath Manjunath, Aydin Behnad, Xianbin Wang and Anestis Dounavis, "Analytical Performance of Millimeter-wave OFDM Systems in Presence of Power Amplifier Nonlinear Distortions", *6th International Conference and Workshop on Computing and Communication*, Oct. 2015